Infiltration Process of Rainfall with Constant Intensity

By Eiichi SHIMOJIMA and Yasuo ISHIHARA

(Manuscript received April 5, 1984)

Abstract

In order to disclose the infiltration process of rainfall into the ground, the infiltration phenomenon is investigated theoretically and experimentally under the conditions that the homogeneous sand layer is bounded at its lower boundary and initially has a uniform moisture profile, and that the rainfall with constant intensity continues. After finding out the approximate solution for a set of fundamental equations with respect to the movement of water and pore-air in the layer, the criterion of ponding on the sand surface, the moving velocity of wetting front, the equation of infiltration rate and so on are presented in comparison with the results of experiment.

1. Introduction

At the initial stage of rainfall, all of the falling water penetrates downwards displacing the pore-air in the unsaturated soil. Thereafter, however, if the rainfall intensity becomes higher beyond the value, which is called the rate of infiltration capacity, ponding of water appears on the ground and only a fraction of rain-water penetrates. Along the mountainuous slope, when such a phenomenon occurs, the ponding water changes to the so-called lateral flow. Such a flow, which forms the surface runoff and constitutes the dominant component of flood runoff, often seems to cause surface erosion or debris flow. And some part of the penetrating water into soil is supplied to the ground water.

Such an infiltration process, which plays a very important role in hydrologic cycle takes place in the limited domain between a land surface and a rock surface or a ground water surface. From a phenomenological point of view, the infiltration can be considered in short as the two phases flows of water and pore-air through porous media. The elucidation of this process was not been done by so many researchers. In our previous paper (1983)[1] on the infiltration process under the condition that water was supplied with constant depth on the surface of sand layer bounded at the bottom from the beginning of infiltration, that is on the ponded infiltration, it was made clear that the upward flow of pore-air and its pressure play an important role on, for example, the downward flow of penetrating water and the rate of infiltration. However, it is considered that the infiltration process by rainfall shows a somewhat different figure from that of ponded infiltration, because all rainwater penetrates into sand layer at the early stage of rainfall but it seems that, after some time has elapsed, a fraction of rainfall begins to pond on the sand surface and so a part of the pore-air is trapped unmoved.

Ishihara, Takagi and Baba (1966)[2] found out the following by undertaking the experiment under the condition that the layer is made of air-dried sand, homogeneous and bounded at the lower boundary, and that the rainfall intensity continues with a constant intensity. The criterion of whether or not ponding on the sand surface appears till the wetting front reaches the bottom of a layer is given by the rainfall intensity of about 3/10–4/10 times of the saturated hydraulic conductivity of sand. Although the description of the phenonenon is qualitative, it was shown that the air pressure ahead of the wetting front in the case having the possibility of ponding grows greater in comparison with that in the case of the non-possibility, and as the time approaches the ponding time, the pressure increases remarkably.

McWhorter (1971)[3] found out by theoretically analyzing the basic equation of movement for water and pore-air that the critical rainfall intensity mentioned above is consistent with the maximum value of the function $K(\theta)K_a(\theta)/\{K(\theta)+K_a(\theta)\}$, where $K(\theta)$ is the hydraulic conductivity and $K_a(\theta)$ the permeability of pore-air, though only a sufficient condition for ponding is considered in this analysis. Further, it was found by undertaking the detail experiment under the same condition of Ishihara and others, that the velocity of a particular saturation is approximately constant during constant rate infiltration. And he theoretically obtained the equation determining the moisture profile by using this experimental evidence, and showed through his research thereafter (1975)[4] that this equation correspnods to the solution of second approximation of the basic equations used in a Parlange's sense.

Phuc and Morel-Seytoux (1972)[5], Sonu and Morel-Seytoux (1976)[6] studied the infiltration process of the rainfall with assumed hyetograph into a homogeneous layer through the numerical calculation of the basic equations of movement for both phases by the finite difference method and the Brustkern and Morel-Seytoux method, respectively. However, the interesting results obtained were not compared with, for example, the experimental ones.

In spite of such a excellent research, there remains the following problems: the critical rainfall intensity for ponding, the process which develops into the ponding condition, the relation between the change of pore-air pressure and the rainfall intensity, the change of infiltration capacity with time, and others.

In this paper, in order to clarify the infiltration process of rain-water into the ground, such a process wherein rain-water of a constant intensity infiltrates into a homogeneous layer which initially had a uniform moisture profile is investigated. That is, by recognizing the infiltration phenomenon as the representation caused by the flow of water and pore-air, the infiltration process, firstly before ponding occurs, is explored theoretically and experimentally, especially by paying attention to the ponding condition. Secondarily, the process after ponding occurs is also explored by comparing it with the situation before ponding and by referring to the result of the ponded infiltration[1]. Finally, by referring to the result obtained above, a simplified equation for defining the rate curve of infiltration capacity is proposed.

2. Theoretical analysis

(1) Boundary and initial conditions

Let us assume that the infiltration field, *i.e.*, the stratum is homogeneous and bounded at the bottom. The moisture profile is initially uniform. The pore-air is initially at atmospheric pressure. The rainfall continues with a constant intensity. Under the condition of no ponding on the surface of stratum, that is, the rainfall intensity being less than the rate of infiltration capacity, the boundary conditions are mathematically given by

$$v = q = \text{constant} \qquad \text{at } x = 0 \qquad\qquad (1)$$

$$p_a \approx 0 \qquad\qquad\qquad \text{at } x = 0 \qquad\qquad (2)$$

$$v = 0 \qquad\qquad\qquad \text{at } x = L \qquad\qquad (3)$$

$$v_a = 0 \qquad\qquad\qquad \text{at } x = L \qquad\qquad (4)$$

where x is the vertical co-ordinate being positive in a gravitational direction and having an origin on the surface of stratum, L the thickness of stratum, v the filter velocity of water, v_a the filter velocity of pore-air, p_a the air pressure in water head showing the increment over the atmospheric pressure, and q the rainfall intensity. And, the initial condition is given by

$$\theta = \theta_0 = \text{constant} \qquad \text{at } t = 0 \qquad\qquad (5)$$

$$p_a = 0 \qquad\qquad\qquad \text{at } t = 0 \qquad\qquad (6)$$

where t is the time and θ the volumetric moisture content.

(2) Fundamental equations

According to our research[1] on the ponded infiltration of a constant water depth into a homogeneous sand layer, under the conditions from Eq. (3) to Eq. (6), the the following was shown.

1. The moisture profile is composed of a quasi-saturated zone and an unsaturated zone. The quasi-saturated zone begins to be formed just beneath the sand surface, when the ponding condition is satisfied on the sand surface, and then develops downwards. However, as time goes by, its development becomes weaker and finally the lower boundary of the zone reaches a specified position being of relatively shallow depth. On the other hand, the unsaturated zone ahead of the quasi-saturated zone continues to develop accompanied by the downward advancement of wetting front.

2. Although the infiltration process is strictly discontinuous because of an intermittent escape of pore-air from the sand surface, such a process can be analyzed as continuous on the average. The movement of water and pore-air obeys the law of Darcy's type in the quasi-saturated zone and the generalized Darcy's law in the unsaturated zone.

We call the ponded infiltration under the condition mentioned above simply as ponded infiltration in this paper.

(a) unsaturated zone

While the moisture content near the upper boundary of the layer does not increase to a large amount, $i.e.$, near saturation, it is considered from the result of the ponded infiltration that water and pore-air throughout the entire domain of an unsaturated layer obeys the generalized Darcy's law.   So, the equations of motion for water and air are given by

$$v = -D\frac{\partial \theta}{\partial x} + K \cdot \left(1 - \frac{\partial p_a}{\partial x}\right) \tag{7}$$

and

$$v_a = -K_a \cdot \left(\frac{\partial p_a}{\partial x} - \frac{\rho_a}{\rho_w}\right), \tag{8}$$

respectively, where

$$D(\theta) = K(\theta) \cdot \frac{d\psi}{d\theta}, \tag{9}$$

$$\psi = p_w - p_a \tag{10}$$

and K is the hydraulic conductivity, D the moisture diffusivity, K_a the permeability of pore-air, ρ_w the density of water, ρ_a the density of air. p_w is the water pressure head, and ψ the capillary potential and to be determined uniquely by θ.

The equations of continuity for water and pore-air are given by

$$\frac{\partial \theta}{\partial t} + \frac{\partial v}{\partial x} = 0 \tag{11}$$

and

$$\frac{\partial \rho_a(\theta_{sat} - \theta)}{\partial t} + \frac{\partial \rho_a v_a}{\partial x} = 0, \tag{12}$$

respectively, where θ_{sat} is the volumetric moisture content in saturation.

Assuming that pore-air is the perfect gas and changes in the isothermal process, the state equation for air is given by

$$\rho_a = C \cdot (P_{a0} + p_a) = C \cdot P_a \tag{13}$$

where C is a numerical consatnt, P_{a0} the atmospheric pressure and $P_a = P_{a0} + p_a$.

Therefore, the following relation can be derived from the set of fundamental equations for the unsaturated zone, Eqs. (7), (8), (11), (12) and (13), by using the boundary condition at $x = L$, Eq. (3) and Eq. (4), under the condition that saturation does not appear in the porous media on the bottom of layer.

$$\frac{\partial p_a}{\partial x} = -\frac{AD}{K}\frac{\partial \theta}{\partial x} - A\varepsilon + \frac{\rho_a}{\rho_w} + A\left(1 - \frac{\rho_a}{\rho_w}\right) \tag{14}$$

where

$$\varepsilon = \int_x^L (\theta_{sat} - \theta) \frac{\partial P_a}{\partial t} dx \Big/ K\bar{P}_a , \tag{15}$$

$$\bar{P}_a(t) = P_a(x, t) - \varDelta p_a(x, t) , \tag{16}$$

$$|\varDelta p_a| / \bar{P}_a \ll 1 , \tag{17}$$

$$A(\theta) = \frac{K}{K + K_a} \tag{18}$$

Here, in order to find out an approximate solution of Eq. (7), Eq. (8), Eq. (11), Eq. (13) and Eq. (14), let us assume that the terms ρ_a/ρ_w and $A(\varepsilon + \rho_a/\rho_w)$, in Eq. (14), can be ignored in comparison with the others as done in our previous paper[1]. Then, Eq. (14) becomes as follows:

$$\frac{\partial p_a}{\partial x} = -\frac{AD}{K} \frac{\partial \theta}{\partial x} + A \tag{19}$$

And, the filter velocity of water, Eq. (7), is also approximated by

$$v = -D(1-A)\frac{\partial \theta}{\partial x} + K(1-A) \tag{20}$$

For convenience of obtaining the solution, converting the independent variables from x and t to θ and t under the assumption that θ is a single-valued function of x at t, Eq. (20), Eq. (19) and the continuity equation of water Eq. (11) are rewritten as

$$v = -D(1-A)\Big/\frac{\partial x}{\partial \theta} + K(1-A) , \tag{21}$$

$$\frac{\partial p_a}{\partial \theta}\Big/\frac{\partial x}{\partial \theta} = -\frac{AD}{K}\Big/\frac{\partial x}{\partial \theta} + A \tag{22}$$

and

$$-\frac{\partial x}{\partial t} = \frac{\partial v}{\partial \theta} , \tag{23}$$

respectively. Let us call Eq. (21) to Eq. (23) as the approximate fundamental equations for the unsaturated zone. These equations, of course, must be used excluding the unsaturated zone of $\partial x/\partial \theta > 0$.

(b) quasi-saturated zone

In the so-called unconfined infiltration under the same condition as ours, except with not a solid but a screen bed, the following is well-known[7]. When ponding begins to occur on the surface of $x=0$, the capillary potential at $x=0$ becomes zero. Since, on the other hand, when the growing moisture content at $x=0$ gets to θ_{sat} from a smaller value, ideally speaking, the capillary potential at $x=0$ is defined by the water entry value being negative, it must take a certain time till the potential reaches from the water entry value to zero. In this duration caused by the characteristic curve representing the relation between the moisture content and the capillary

potential of the layer, the saturated zone is formed downwards from the upper bound-
ary of the layer. It is common-sense to consider that a process similar to such a
forming process of a saturated zone appears in our case as well, and that indeed the
quasi-saturated zone corresponds to such a saturated zone.

So, before ponding, if we assume that the quasi-saturated zone is formed down-
wards from the upper boundary of a layer, according to the similarity to the ponded
infiltration, the motion of water and pore-air in that zone obey the law of Darcy's
type given by[1]

$$\hat{v} = \hat{K} \cdot \left(1 - \frac{p_{w1} - p_{w0}}{x_1} \right) \tag{24}$$

and

$$\hat{v}_a = -\hat{K}_a \cdot \frac{p_{a1} - p_{a0}}{x_1}, \tag{25}$$

respectively, where $\hat{v}$ is the filter velocity of water, $\hat{K}$ the equivalent hydraulic con-
ductivity, x_1 the thickness of the quasi-saturated zone, that is, the x-ordinate of the
lower boundary of that zone, p_{w0} the water pressure head at $x=0$, p_{w1} the water pres-
sure head at $x=x_1$, $\hat{v}_a$ the filter velocity of pore-air, $\hat{K}_a$ the equivalent permeability of
pore-air, p_{a0} the air pressure in water head at $x=0$, and p_{a1} the air pressure in water
head at $x=x_1$.

(3) Criterion of ponding

Before discussing the criterion of ponding, let us derive the formal expression of
solution with respect to the moisture content of the unsaturated zone.

Let us assume that, during a constant rainfall, there remains, at least, the domain
of $\theta=\theta_0$ ahead of the wetting front, that is, the effect of the reflection of a down-
ward penetrating water by the lower boundary of a layer on the advancing wetting
front is negligible.   According to Philip (1973)[8], let us define the following function.

$$F = \frac{v - v_0}{v_s - v_0} \tag{26}$$

where the suffix s means the value at $x=0$ and the suffix 0 means the value at $\theta=\theta_{0+}$.

Because of the stage before ponding, v_s is obviously equal to the rainfall intensity,
q, from Eq. (1). Since

$$1 \bigg/ \frac{\partial x}{\partial \theta} \to 0 \qquad \text{at } \theta \to \theta_{0+} \tag{27}$$

by the initial condition of Eq. (5), v at $\theta=\theta_{0+}$ in Eq. (21) becomes

$$v_0 = \{K(1-A)\}_0 \tag{28}$$

Therefore, the function F can be expressed as

$$F(\theta, t) = \frac{-D(1-A)\Big/\frac{\partial x}{\partial \theta}+K(1-A)-K_0(1-A_0)}{q-K_0(1-A_0)} \tag{29}$$

where F satisfies the following conditions.

$$F_s = 1 \tag{30}$$

$$F_0 = 0 \tag{31}$$

$$1 \geq F \geq 0 \tag{32}$$

Since θ_s depends on t, the F is also the function of θ and θ_s.

Rearranging Eq. (29) with respect to $\partial x/\partial \theta$, we get

$$\frac{\partial x}{\partial \theta} = \frac{D(1-A)}{K(1-A)-qF-K_0(1-A_0)(1-F)} \tag{33}$$

Integrating Eq. (33) with respect to θ, the moisture profile is formally given by

$$x = -\int_\theta^{\theta_s} \frac{D(1-A)}{K(1-A)-qF-K_0(1-A_0)(1-F)} d\theta \tag{34}$$

After partially differentiating Eq. (34) with respect to t, applying Eq. (30) to it, we get

$$\frac{\partial x}{\partial t} = -\frac{d\theta_s}{dt}\left[\left\{\frac{D(1-A)}{K(1-A)-q}\right\}_s + \int_\theta^{\theta_s} \frac{D(1-A)\{q-K_0(1-A_0)\}\frac{\partial F}{\partial \theta_s}}{\{K(1-A)-qF-K_0(1-A_0)(1-F)\}^2} d\theta\right] \tag{35}$$

Since $\partial x/\partial t$ given by Eq. (35) must satisfy the continuity equation for water, Eq. (23), after integrating Eq. (35) with respect to θ from θ_{0+} to θ_s, using Eq. (1) and Eq. (28), we get

$$\frac{d\theta_s}{dt} = -\{q-K_0(1-A_0)\}\Big/\left[\left\{\frac{(\theta-\theta_0)D(1-A)}{K(1-A)-q}\right\}_s\right.$$
$$\left. + \int_{\theta_0}^{\theta_s} d\theta \int_\theta^{\theta_s} \frac{D(1-A)\{q-K_0(1-A_0)\}\frac{\partial F}{\partial \theta_s}}{\{K(1-A)-qF-K_0(1-A_0)(1-F)\}^2} d\theta\right] \tag{36}$$

Eq. (36) gives the formal expression of $\theta_s(t)$.

Introducing Eq. (36) into Eq. (35), the moving velocity of particular saturation is given formally by

$$\frac{\partial x}{\partial t} = \{q-K_0(1-A_0)\}$$

$$\times \frac{\left\{\dfrac{D(1-A)}{K(1-A)-q}\right\}_s + \displaystyle\int_\theta^{\theta_s} \dfrac{D(1-A)\{q-K_0(1-A_0)\}\frac{\partial F}{\partial \theta_s}}{\{K(1-A)-qF-K_0(1-A_0)(1-F)\}^2} d\theta}{\left\{\dfrac{(\theta-\theta_0)D(1-A)}{K(1-A)-q}\right\}_s + \displaystyle\int_{\theta_0}^{\theta_s} d\theta \displaystyle\int_\theta^{\theta_s} \dfrac{D(1-A)\{q-K_0(1-A_0)\}\frac{\partial F}{\partial \theta_s}}{\{K(1-A)-qF-K_0(1-A_0)(1-F)\}^2} d\theta} \tag{37}$$

Integrating Eq. (22) which is multiplied by $\partial x/\partial \theta$ with respect to θ and using Eq. (33), the profile of pore-air pressure is formally given by

$$p_a = p_a(\theta_s, t) + \int_\theta^{\theta_s} \frac{AD}{K} d\theta - \int_\theta^{\theta_s} \frac{AD(1-A)}{K(1-A)-qF-K_0(1-A_0)(1-F)} d\theta \quad (38)$$

where $p_a(\theta_s, t)$ is p_a at $x=0$ and obeys Eq. (2).

Now, let us advance the discussion with respect to the criterion of ponding. The condition that, before the wetting front reaches the bottom of a layer, ponding occurs on the upper boundary of that layer, can be considered to be equivalent to such a condition that the moisture content at the upper boundary of the layer, θ_s, continues to increase. Since Eq. (21) does not contain the effect of the thickness of layer because ε term in Eq. (14) is neglected, this equation is valid for an arbitrary thickness of layer in a mathematical sense.

Then, in order to find out the criterion of ponding, let us consider the sufficiently thick layer.

Fig. 1 shows the relations between A and θ, and $K(1-A)$ and θ for a sand used in experiments, Sand K-7 mentioned in **3.(1)**. We denote the moisture content at the maximum values of $K(1-A)$ and $\{K(1-A)-K_0(1-A_0)\}/(\theta-\theta_0)$ as θ_c and θ_c', respectively, though in this figure the initial moisture content, θ_0, is taken as zero. Furthermore, various quantities at $\theta=\theta_c$ and $\theta=\theta_c'$ are shown by adding the suffix c and c', respectively.

i)   the case of $q<\{K(1-A)\}_c$

Since the intensity of rainfall, q, is weaker than $\{K(1-A)\}_c$, the line, $q=$constant, intersects at two points with the $K(1-A)\sim\theta$ curve as known from **Fig. 1**.
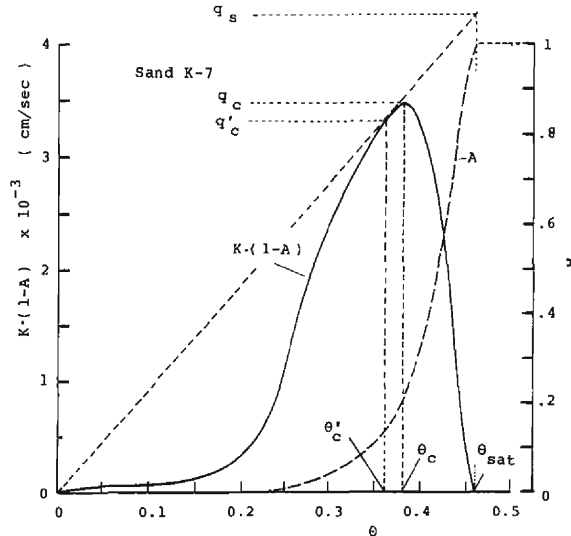

Fig. 1   Relation between $K(1-A)$ or A and moisture content, θ, in the case of Sand K-7, where the value of λ in Eq. (56) is taken as 1.8

Let us denote the lesser of the moisture content at two intersections as $\bar{\theta}$ which is, of course, smaller than θ_c.

While the value of θ_s continues to increase from the initial value, θ_0, at the early stage of rainfall, the denominator in the right side of Eq. (33) has obviously a negative sign because of $D(1-A)>0$ and $\partial\theta/\partial x<0$. So, it is known that, even when θ_s reaches $\bar{\theta}$, the wetting front has not advanced to a sufficient depth. However, when θ_s approaches $\bar{\theta}$, the denominator at $\theta=\theta_s$ becomes zero due to Eq. (30). This means that $\partial\theta/\partial x\to0$, that is, the wetting front must have advanced sufficiently with a long elapsed time. At the time, furthermore, the rate of penetration of water through the upper boundary of the layer is given by q from Eq. (21). It can be concluded from the above consideration that, when θ_s approaches $\bar{\theta}$, $d\theta_s/dt$ becomes zero and, as a result, ponding does not appear.

After all, under the condition of $q<\{K(1-A)\}_c$, θ_s cannot increase over $\bar{\theta}$ ($<\theta_c$) and so ponding cannot occur.

ii)　the case of $q>\{K(1-A)\}_c$

Before discussing the criterion of ponding in this case, the several equations which are necessary to develop our considerations are described.

According to the result of the ponded infiltration[1], under the condition that the wetting front is advancing with an unchangeable profile and a constant velocity into the homogeneous layer satisfying Eq. (3) and Eq. (4), the following relation is obtained through Eq. (21) to Eq. (23).

$$\zeta-\zeta_*^{\it\Delta} = -\int_\theta^{\theta_*-\Delta_*} \frac{D(1-A)}{K(1-A)-K_0(1-A_0)-\dfrac{\theta-\theta_0}{\theta_*-\theta_0}\{K_*(1-A_*)-K_0(1-A_0)\}}\,d\theta \quad (39)$$

$$\omega_* = \frac{K_*(1-A_*)-K_0(1-A_0)}{\theta_*-\theta_0} \quad (40)$$

$$\theta_*\le\theta_c' \quad (41)$$

$$p_a-(p_a)_*^{\it\Delta} = \int_\theta^{\theta_*-\Delta_*} \frac{AD}{K}\,d\theta$$

$$-\int_\theta^{\theta_*-\Delta_*} \frac{AD(1-A)}{K(1-A)-K_0(1-A_0)-\dfrac{\theta-\theta_0}{\theta_*-\theta_0}\{K_*(1-A_*)-K_0(1-A_0)\}}\,d\theta \quad (42)$$

where the wetting front is in the range of $\theta_0<\theta<\theta_*$, being $d\zeta/d\theta\to0$ at $\theta=\theta_{*-}$, ω_* the moving velocity of wetting front, Δ_* a certain small positive value, ζ the moving co-ordinate with the velocity of ω_*, $\zeta_*^{\it\Delta}$ ζ at $\theta=\theta_*-\Delta_*$, and $(p_a)_*^{\it\Delta}$ p_a at $\zeta=\zeta_*^{\it\Delta}$. And the suffix $*$ means the quantity at $\zeta=\zeta_{*+}$, i.e., $\theta=\theta_{*-}$. Eq. (39) and Eq. (42) give the relative profile of wetting front and pore-air pressure, respectively.

If the following relation is satisfied in Eq. (21)

$$K(1-A)\gg D(1-A)\Big/\left|\frac{\partial x}{\partial\theta}\right| \quad (43)$$

the continuity equation of water, Eq. (23), is approximated as follows by introducing Eq. (43) into it.

$$\frac{\partial \theta}{\partial t} + \frac{dK(1-A)}{d\theta} \frac{\partial \theta}{\partial x} = 0 \tag{44}$$

The differential equation of Eq. (44) is equivalent to the following relation.

$$\theta = \text{constant} \qquad \text{on} \; \frac{dx}{dt} = \frac{dK(1-A)}{d\theta} \tag{45}$$

Now, we denote the moisture content at the upper boundary of a layer at the ponding time as θ_m, which is expected to be larger than θ_c. In order to find out the criterion of ponding, let us assume that $d\theta_s/dt$ approaches zero and θ_s approaches a certain value, $\theta_{s\infty}$ being smaller than θ_m, with a long elapsed time. Then, it is known from Eq. (34) that, as time goes by, the moisture content, θ'_*, satisfying the relation of $K(1-A) - K_0(1-A_0) - F\{q - K_0(1-A_0)\} = 0$ is possible to appear at a certain depth. This moisture content θ'_* is not equal to $\theta_{s\infty}$ due to Eq. (30) and the condition of $q > \{K(1-A)\}_c$. And, at the stage of $\theta_s \approx \theta_{s\infty}$, the wetting front obviously must have advanced sufficiently deeply. Since the moisture content just behind the deeply advanced wetting front is held constant, θ_* defined by the relations from Eq. (39) to Eq. (42) can be applied to θ'_* or the smallest of θ'_*, being, of course, omitted for the case of $\theta'_* = \theta_0$, if there are several values of θ'_*.

Let us set the plausible condition that, as time goes by, the wetting front advances with an unchangeable profile and a constant velocity. So, the wetting front exists in the range of $\theta_0 < \theta < \theta_*$. The moisture content in the range of $\theta_{s\infty} > \theta > \theta_*$ must satisfy the condition of Eq. (43) and the θ_* must be consistent with θ'_c (see **Appendix**).

On the other hand, integrating the continuity equation of water, Eq. (23), with respect to θ, we get the relation, $\int_{\theta'_c}^{\theta_s} \frac{\partial x}{\partial t} d\theta = v_s - v'_c$. Since v_s and v'_c are equal to q and $\{K(1-A)\}'_c$, respectively, the integral is equal to $q - \{K(1-A)\}'_c$. However, since we also get the relation, $\int_{\theta'_c}^{\theta_s} \frac{\partial x}{\partial t} d\theta = \{K(1-A)\}_s - \{K(1-A)\}'_c$ from Eq. (45), both the values of above integral are not equal because of the condition that $[\{K(1-A)\}_s]_{\max} = \{K(1-A)\}_c < q$. That is, the continuity equation of water is not satisfied. This means that the assumption of $d\theta_s/dt \to 0$ and $\theta_s \to \theta_{s\infty}$ with a long elapsed time is unreasonable. Therefore, in the case of $q > \{K(1-A)\}_c$, $d\theta_s/dt$ has a positive sign. It follows that θ_s must continue to increase to θ_m. As a result, ponding can occur at a certain time.

The criterion of rainfall intensity whether ponding appears or not is given by $q = \{K(1-A)\}_c$. Although this value is consistent with the lower critical infiltration

rate in the ponded infiltration[1] (see **3.(2)**), this consistency is physically plausible and reasonable.

(4) Solution by the approximate method

(a) approximate method

The formal solution of the approximate fundamental equation for the unsaturatde zone, Eqs. (34), (36), (37) and (38), contains the unknown function $F(\theta, t)$ or $F(\theta, \theta_s)$. So, F must be determined practically.

Let us use the following iterative method according to Philip and Knight (1974)[9]. At first, let us consider that F in i-th approximation, F_i, is given. The right side of Eq. (37), in which F is replaced by F_i, is represented as $(\partial x/\partial t)_i$. Next, according to the definition of F given by Eq. (29), F in $(i+1)$th approximation, F_{i+1}, is defined by

$$F_{i+1} = \int_{\theta_0}^{\theta} \left(\frac{\partial x}{\partial t}\right)_i d\theta \Big/ \int_{\theta_0}^{\theta_s} \left(\frac{\partial x}{\partial t}\right)_i d\theta \tag{46}$$

And then by repeating these procedures, $F_{i+n}(n \geq 2)$ can be gotten formally. Therefore, if a proper F_N is determined, $\theta_s(t)$ in N-th approximation can be determined by solving Eq. (36). Using $\theta_s(t)$, the profiles of the moisture and the pore-air pressure are determined from Eq. (34) and Eq. (38), respectively.

(b) second approximation

Following Parlange (1972)[10], let us give the following relation as F_1.

$$F_1 = 1 \tag{47}$$

By using Eq. (47) and according to article (**a**), we get easily

$$F_2 = \frac{\theta - \theta_0}{\theta_s - \theta_0} \tag{48}$$

If Eqs. (34), (36), (37) and (38) are expressed by using Eq. (48), these are given by

$$x = -\int_{\theta}^{\theta_s} \frac{D(1-A)}{K(1-A) - K_0(1-A_0) - \{q - K_0(1-A_0)\}\dfrac{\theta - \theta_0}{\theta_s - \theta_0}} \, d\theta \tag{49}$$

$$\frac{d\theta_s}{dt} = -\frac{q - K_0(1-A_0)}{\left\{\dfrac{(\theta - \theta_0)D(1-A)}{K(1-A) - q}\right\}_s - \dfrac{q - K_0(1-A_0)}{\theta_s - \theta_0} \times} $$

$$\overline{\int_{\theta_0}^{\theta_s} d\theta \int_{\theta}^{\theta_s} \frac{\dfrac{\theta - \theta_0}{\theta_s - \theta_0} D(1-A)}{\left[K(1-A) - K_0(1-A_0) - \dfrac{\theta - \theta_0}{\theta_s - \theta_0}\{q - K_0(1-A_0)\}\right]^2} d\theta} \tag{50}$$

$$\frac{\partial x}{\partial t} = \{q - K_0(1-A_0)\} \frac{\left\{\dfrac{D(1-A)}{K(1-A)-q}\right\}_s - \dfrac{q-K_0(1-A_0)}{\theta_s-\theta_0} \times}{\left\{\dfrac{(\theta-\theta_0)D(1-A)}{K(1-A)-q}\right\}_s - \dfrac{q-K_0(1-A_0)}{\theta_s-\theta_0} \times}$$

$$\frac{\displaystyle\int_\theta^{\theta_s} \frac{\dfrac{\theta-\theta_0}{\theta_s-\theta_0}D(1-A)}{\left[K(1-A)-K_0(1-A_0)-\dfrac{\theta-\theta_0}{\theta_s-\theta_0}\{q-K_0(1-A_0)\}\right]^2}d\theta}{\displaystyle\int_{\theta_0}^{\theta_s}d\theta\int_\theta^{\theta_s}\frac{\dfrac{\theta-\theta_0}{\theta_s-\theta_0}D(1-A)}{\left[K(1-A)-K_0(1-A_0)-\dfrac{\theta-\theta_0}{\theta_s-\theta_0}\{q-K_0(1-A_0)\}\right]^2}d\theta} \tag{51}$$

$$p_a = p_{as} + \int_\theta^{\theta_s}\frac{AD}{K}\,d\theta - \int_\theta^{\theta_s}\frac{AD(1-A)}{K(1-A)-K_0(1-A_0)-\dfrac{\theta-\theta_0}{\theta_s-\theta_0}\{q-K_0(1-A_0)\}}\,d\theta \tag{52}$$

These equations are the solutions of second approximation. The expression of the solutions of further higher orders of approximation can be obtained mechanically but tediously.

Eq. (49) and Eq. (50) are equivalent to the equations in the second approximation obtained independently by Mcwhorter[4] through Parlage's method.

(c) accuracy of the solution of second approximation

It is known easily from Eq. (49) and Eq. (52) that the solution of the second approximation is characterized by the following condition.

$$K(1-A)-K_0(1-A_0)-\{q-K_0(1-A_0)\}\frac{\theta-\theta_0}{\theta_s-\theta_0} \to 0 \tag{53}$$

In other words, since the value of x given by Eq. (49) approaches infinity when Eq. (53) is satisfied, the wetting front goes down to a deep enough position. This means that it takes an infinite time to satisfy such a condition.

Now, in **Fig. 1**, since θ_s increases from left to right when a rainfall continues, the condition given by Eq. (53) is satisfied on the $K(1-A)$-curve between θ_0 and θ_c' and on the tangent line between θ_c' and θ_{sat}. On the other hand, as shown already in section (3), in the case of $q<\{K(1-A)\}_c$, θ_s can approach the $K(1-A)$-curve and no ponding appears, and in the csae of $q>\{K(1-A)\}_c$, θ_s beocmes θ_m and ponding appears. It is, therefore, convenient to examine the accuracy of the solution of second approximation in the four regions of as shown in **Fig .1**, that is $q<q_c'$, $q_c'<q<q_c$, $q_c<q<q_s$ and $q>q_s$, where $q_c'=\{K(1-A)\}_c'$, $q_c=\{K(1-A)\}_c$ and $q_s=[\{K(1-A)\}_c'-K_0(1-A_0)]\cdot(\theta_{sat}-\theta_0)/(\theta_c'-\theta_0)+K_0(1-A_0)$. In this figure, θ_0 is set zero as mentioned before.

The case of $q<\{K(1-A)\}_c'$ In this case, the value of θ_s of the approximate solution can increase from θ_0 to $\tilde{\theta}$ on the $K(1-A)$-curve after a long elapsed time. Therefore, a high level of accuracy of the solution is expected, at least, after enough time has passed. The advancing wetting front may be approximated as follows:

$$x(\theta, t) = \omega_* \cdot (t-t_0) + \chi_0(\theta) \tag{54}$$

where t_0 is the time when $\partial x/\partial t$ becomes about ω_* given by Eq. (40) in which θ_* is replaced by $\tilde{\theta}$, and $\chi_0(\theta)$ is the moisture profile at $t=t_0$ and corresponds to $\zeta - \zeta_*^4$ in Eq. (39). So, using Eq. (49) and Eq. (54), Eq. (52) is rewritten as

$$p_a(\theta, t) \approx p_a(\theta_s - \Delta_*, t) + \left\{ \left[\int_\theta^{\theta_* - \Delta_*} \frac{AD}{K} d\theta - A(\theta_s - \Delta_*) \cdot \chi_0(\theta) \right] \right. \\ \left. + A(\theta_s - \Delta_*) \cdot \omega_* \cdot (t-t_0) \right. \tag{55}$$

where Δ_* is the small quantity when the range of integral in Eq. (49), (θ, θ_s), is divided into $(\theta, \theta_s - \Delta_*)$ and $(\theta_s - \Delta_*, \theta_s)$.

Since $p_a(\theta_s - \Delta_*, t)$ is nearly equal to zero by the condition of Eq. (2), it is known that, according to the time elapsed, the pore-air pressure at the point having the particular θ along the wetting front reaches the condition so that it increases linearly with time and its rate of change is independent of θ.

The case of $\{K(1-A)\}_c' < q < \{(K(1-A)\}_c$ In this case, the value of θ_s of the approximate solution cannot approach θ on the $K(1-A)$-curve. Even with a long elapsed time, no ponding will appear. Since, however, the difference between the $K(1-A)$-curve and the tangent line is small, the accuracy of the approximate solution is expected to hold in some degree.

The case of $\{K(1-A)\}_c < q < [\{K(1-A)\}_c' - K_0(1-A_0)] \cdot (\theta_{sat} - \theta_0)/(\theta_c' - \theta_0) + K_0(1-A_0)$ In this case, the value of θ_s of the approximate solution approaches θ on the tangent line after the long elapsed time and no ponding appears. For this range of rainfall intensity, q, however, it is already known that ponding occurs and θ_s becomes θ_m. So some error is contained in the approximate solution, especially, in the occurrence condition of ponding.

The case of $q > [\{K(1-A)\}_c' - K_0(1-A_0)] \cdot (\theta_{sat} - \theta_0)/(\theta_c' - \theta_0) + K_0(1-A_0)$ It is known from Eq. (49) or Eq. (50) that the value of θ_s of the approximate solution can continue to increase to θ_m. The solutions in this case satisfy the condition that ponding can appear as expected in section (3). Since the solution does not contain the limiting state showing characteristic properties in the range of $q > \{K(1-A)\}_c$ as mentioned in section (3), we cannot investigate the degree of accuracy of the approximate solution. The approximate solution in this case will be examined from a different view of point as described below.
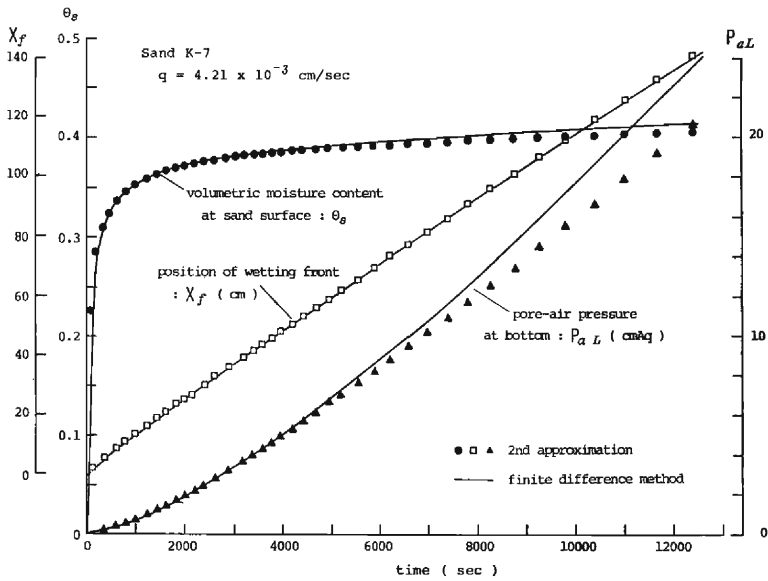
(d) comparison with the solution by the finite difference method

Let us examine the degree of accuracy of the approximate solution by using the finite difference method for the original fundamental equation. The Newton-Raphson method was applied to obtain the finite difference scheme.

Fig. 2(a) and **(b)** show the comparison concerning the moisture content at $x=0$, θ_s, the depth of the wetting front, x_f, and the pore-air pressure at $x=L$, p_{aL}, where the layer is made of Sand K-7 shown later in **Fig. 3**, the initial moisture content has very small value, and the thickness of layer is 170 cm. The p_{aL} of the approximate
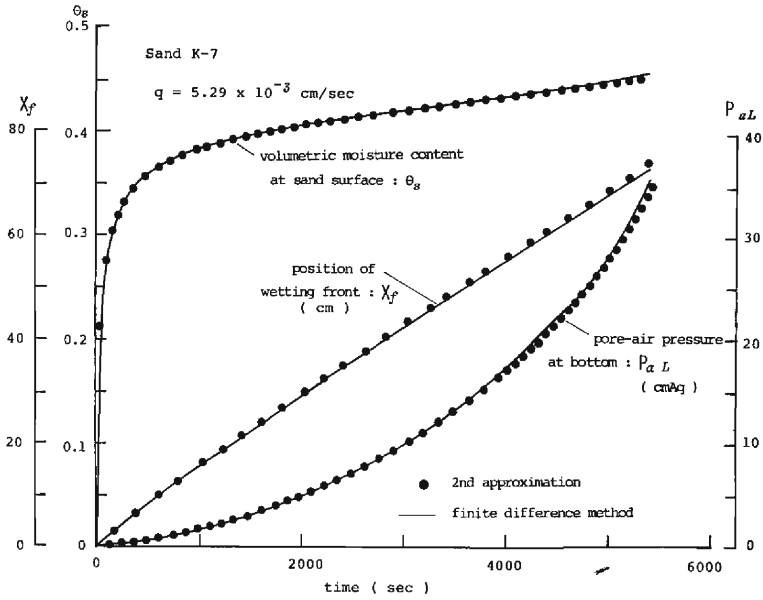
Fig. 2   Comparison of the calculated values by approximate solution with ones
         by finite difference method
         (a) $q=5.29 \times 10^{-3}$ cm/sec in Sand K-7
         (b) $q=4.21 \times 10^{-3}$ cm/sec in Sand K-7

solution is shown by the value of Eq. (52) at $\theta \to 0_+$. The x_f in both solutions is shown by the value of x with respect to $\theta = 0.2$. The rainfall intensity is a little greater than $\{K(1-A)\}_c' \theta_{sat}/\theta_c'$ in the former figure, and is intermediate between $\{K(1-A)\}_c$ and $\{K(1-A)\}_c' \theta_{sat}/\theta_c'$ in the latter figure. It seems from **Fig. 2(a)** that both solutions agree well. It seems from **Fig. 2(b)** that, although the values of θ_s and p_{aL} agree well till θ_s becomes about 0.39 (being about $\dot{\theta}_c$), after that, as time goes by, the values of approximate solutions depart from those by the finite difference method. However, in spite of these departures, both x_f terms are seemed to agree well. These departures are especially considered to be caused by the degree of accuracy of the approximation.

The following is concluded from article (**c**) and the results of comparison, though θ_m in calculations is taken as θ_{sat}.

In the case that q is more than $\{K(1-A)\}_c' \theta_{sat}/\theta_c'$ but is not sufficiently great, the approximation of Eq. (14) by Eq. (19) seems to be possible and the approximate solution is of high accuracy. However, in the case when q is especially great, the application of Eq. (19) will remain a problem with the elapsed time because, as known also from **Fig. 2** and **Fig. 5** shown later, the change rate of pore-air pressure increases greatly with time.

In the case of $\{K(1-A)\}_c < q < \{(K(1-A)\}_c' \theta_{sat}/\theta_c'$, the application of Eq. (19) is considered to be possible. However, since θ_s never increases to θ_{sat}, the use of the approximate solution is not available over the large θ_s. So, the application of this solution may be limited in range till θ_s becomes θ_c.

In the case of $\{K(1-A)\}_c' < q < \{K(1-A)\}_c$, according as θ_s approaches the point on the tangent line, the degree of accuracy of the approximate solution becomes lower.

In the case of $q < \{K(1-A)\}_c'$, we did not try the comparison. However, the application of Eq. (19) may be possible because the change rate of pore-air pressure does not become obviously so great compared with the case of **Fig. 2(a)** (see **Figs. 15(b)** and **17**). So, from the result obtained in article (**c**) the approximate solution can be available with high accuracy, except for only a very deep layer.

After all, taking care of the range of application mentioned above, the approximate solution can be applied usefully instead of the solution of the finite difference method.

In the calculation by the finite difference method for **Fig. 2(a)** and (**b**), $\Delta x = 1$ cm and $\Delta t = 0.5$ sec were used as grid difference. The calculating times by FACOM 230-48 are very long, that is, about 13 hrs for **Fig. 2(a)** and 24 hrs for **Fig. 2(b)**. However, in the case of the approximate solution, it takes only about $1/30$ of the time taken by the finite difference method.

3. Experiments and several considerations

(1) Apparatus and method of the experiment

A homogeneous layer is made of two kinds of naturally air-dried sand, Sand K-7
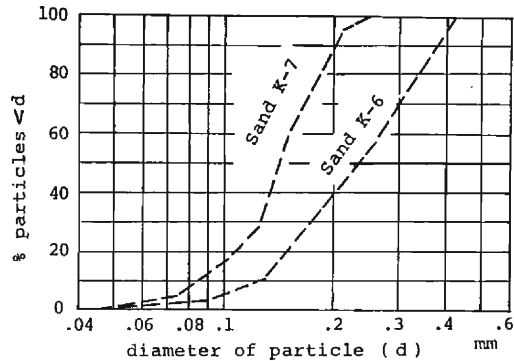
Fig. 3 Distribution of particle-size

and Sand K-6 shown in **Fig. 3**, being inserted into a lucite cylinder of 18.5 cm in inner diameter and 170 cm in length with a bottom solid plate. Around the upper part of the cylinder, a receiver for the water overflowing from its upper edge is installed. The upper boundary of a layer, *i.e.*, the sand surface is horizontal and 0.5 cm deep under the upper boundary of the cylinder. So, the layer is 169.5 cm in thickness, and when ponding occurs on the sand surface, its maximum depth is nearly equal to 0.5 cm. The degree of compactness of sand layer is 1.41–1.39 gr/cm^3 for Sand K-7 and 1.43–1.42 gr/cm^3 for Sand K-6, and the porosity is almost 0.46 in both.

Water supply simulating rainfall is done on the sand surface as uniformly as possible with a constant intensity by the following apparatus. The apparatus is made of four parts connected to each other with vinyl tubes, that is, in order of flow direction, a water tank, a pump, a flow meter and a thin cylindrical case. This case is 18.5 cm in inner diameter, 5 cm in depth and bounded by plates at both boundaries. On the upper plate, a cock is connected and, on the bottom plate, many injection needles of 0.8 mm in inner diameter are installed. The flow meter has also the faculty to make the flow stable. The sand surface is covered with a fine mesh to protect it from the impact of raindrops before ponding.

The moisture content and the pore-air pressure are usually measured during an experiment. Especially, after ponding occurs on the sand surface and then its water overflows from the upper edge of the cylinder, the infiltration rate is measured. The moisture content is measured by an electric capacitance method (see **reference** 1)). The pore-air pressure is measured by a pressure gauge set on the side wall near the bottom of a layer. The infiltration rate is estimated by subtracting the discharge of overflowing water mentioned above from the intensity of the water supply.

Experiments are carried out in an air conditioned room at about 21°C, till the wetting front reaches the bottom of a layer.

(2) **Comparison of the experimental result with the calculated one**

The calculated result mentioned here is by the approximate solution, that is,

the solution in the second approximation in **2.(4)**.

(a) **effect of the permeability of pore-air on the approximate solution**

The permeability of pore-air, $K_a(\theta)$, for the experimental sand is not measured. So, before comparison, let us examine the effect of the permeability of the pore-air on the calculated value of approximate solution, in advance. We assume the function of $K_a(\theta)$ as follows.[11]

$$K_a(\theta) = K(\theta_{sat}) \frac{\mu_w}{\mu_a} \cdot \left(1 - \frac{\theta}{\theta_{sat}}\right)^{\lambda} \tag{56}$$

where μ_w and μ_a are the coefficient of viscosity of water and pore-air, respectively, and λ a positive numerical constant. The effects of the parameter λ in Eq. (56) on the depth of the wetting front, the pore-air pressure ahead of the wetting front and the moisture content at the sand surface are shown in **Fig. 4**. The layer consists
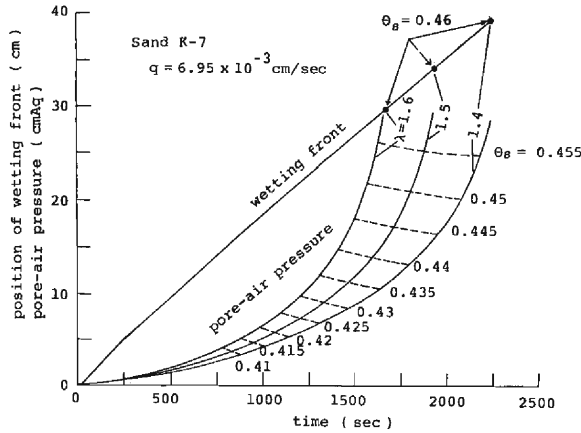
Fig. 4 Changes of the calculated depth of wetting front, the pore-air pressure ahead of wetting front and the moisture content at a sand surface, due to parameter λ

of Sand K-7, the rainfall intensity is $q=6.95 \times 10^{-3}$ cm/sec being in the condition of $q > \{K(1-A)\}'_c \theta_{sat}/\theta'_c$. Furthermore, the wetting front and the pore-air pressure are represented by $\theta=0.2$ in Eq. (49) and evaluated at $\theta \to 0_+$ in Eq. (52), respectively. The moisture content at $x=0$ is calculated by Eq. (50). The procedure of calculation is explained in **2.(4) (a)**. In this case, the range of the λ-value is referred to the result mentioned in the next article (**b**). Especially, the broken line in this figure is described by the value of the moisture content at $x=0$ as a parameter. Although the difference of the λ-value has great effect upon the pore-air pressure as θ_s increases over $\theta_s \approx 0.42$ (corresponding to about 91% of saturation). In such a stage of θ_s the value of air pressure at the particular value of θ_s seems to be nearly independent of the λ-value. The wetting front seems to advance along an unique line. However, the depth of wetting front at $\theta_s=\theta_{sat}$, shown by a black circle, differs by the λ-value.

### (b)   experiment in which ponding occurs
i)   before ponding
    a.   pore-air pressure

The comparisons between the observed values of pore-air pressure and the calculated ones are shown in **Fig. 5(a)** for Sand K-7 and (**b**) for Sand K-6, where the observed values are described till the time just after ponding occurs.   The λ-value in calculation is selected as the calculated value agrees well with the observed one. The λ-value obtained in various experiments for Sand K-7 is 1.4–1.6 and almost about 1.5.   However, the λ-value for Sand K-6 was scattered over a relatively wide
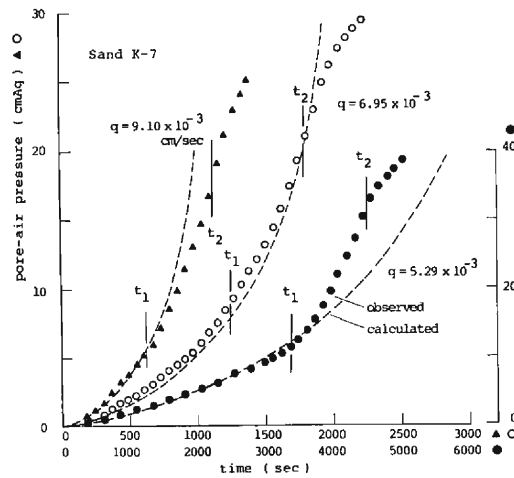
(a)
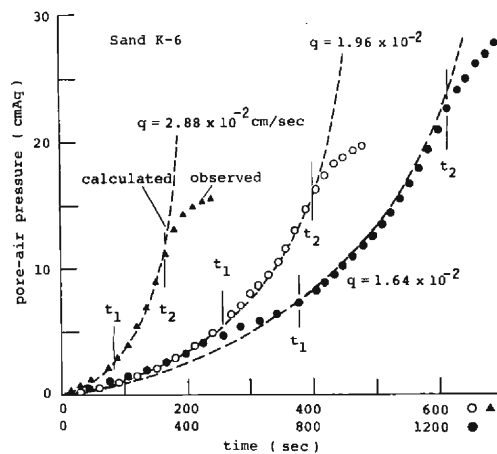
(b)

Fig. 5   Change of the pore-air pressure at the bottom of a layer
    (a)   in the case of Sand K-7
    (b)   in the case of Sand K-6

range, 1.31–2.37 (except one special case, being smaller than 1.9) and an approximate unique value could not be determined as with Sand K-7. The following property of the change of observed pore-air pressure is known from these figures.

1. The pore-air pressure increases in the state of $d^2 p_{aL}/dt^2 > 0$ till a certain time, t_2.

2. From a certain time, t_1, between $t=0$ and $t=t_2$, the pore-air pressure increases remarkably.

Plotting the relation between the depth of wetting front at $t=t_1$ and the pore-air pressure at the same time, we get **Fig. 6**, where a black and a white circle show the cases that ponding was observed and those that ponding was not observed but $d^2 p_{aL}/dt^2$ showed a positive sign, respectively. A group of lines with various values of θ_s as a parameter in this figure is the calculated values when $\lambda = 1.5$. It seems from this figure that the observed values are about between the calculated values of $\theta_s = 0.42$ and $\theta_s = 0.43$, *i.e.*, the degree of saturation is $0.425/0.46 \times 100 = 92\%$, and these obey the straight broken line in this figure. Let us examine the gradient of broken line. From Eq. (34) and Eq. (38), the following relation is obtained.

$$\frac{\partial p_{aL}}{\partial x_f} = \int_{0+}^{\theta_s} \frac{AD(1-A)F}{\{K(1-A)-qF\}^2} d\theta \bigg/ \int_{0+}^{\theta_s} \frac{D(1-A)}{\{K(1-A)-qF\}^2} d\theta \tag{57}$$

where x_f and p_{aL} are x in Eq. (34) and p_a in Eq. (38) at $\theta \to 0_+$, respectively. The
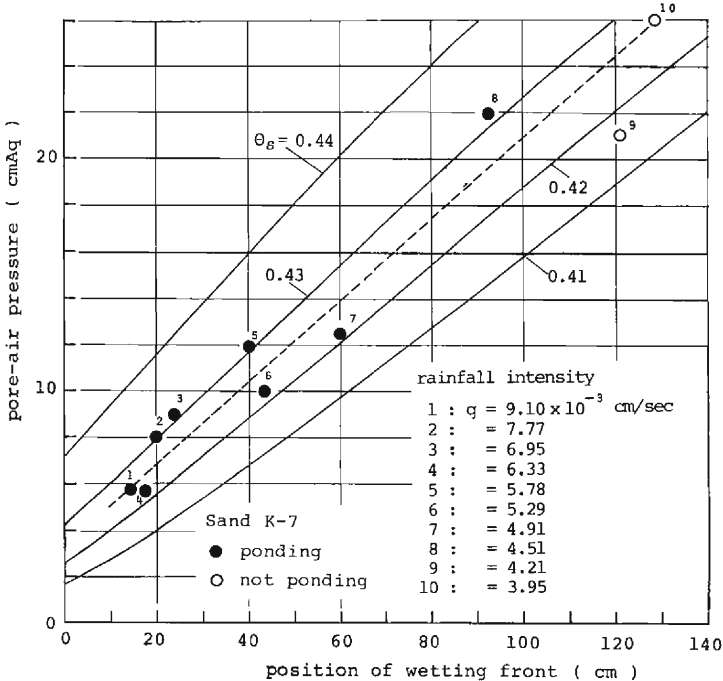

Fig. 6 Relation between the pore-air pressure ahead of wetting front and the depth of wetting front at the time when the pore-air pressure increases abruptly

maximum of rainfall intensity in our experiment is about twice as large as $\{K(1-A)\}_c$. Considering that the maximum value of $D(1-A)$ appears to be about $\theta=\theta_c$ and the shape of profile of $D(1-A)$ is similar to that of $K(1-A)$, and referring to Eq. (48) as the shape of the function F, the integral of the numerator in the right side of Eq. (57) is to be determined at the moisture content in the neighbourhood of θ_c because $\theta_c > \theta_s$. So, $\partial p_{aL}/\partial x_f$ in Eq. (57) can be approximated by $A(\theta_c)$. By using the value, 0.17, of the gradient of the broken line in **Fig. 6**, we can know that the moisture content under the condition of $A(\theta)=0.17$ is equal to that of θ_c, i.e., about 0.39.

Although, in the case of Sand K-6, we could not obtain the relation between the observed value and the calculated one as in **Fig. 6**, it was noted that the observed values scatter nearly around a straight broken line and the value of its gradient is equal to about that in the case of Sand K-7.

After all, when the increasing moisture content at $x=0$ reaches about 90% of saturation, the pore-air pressure begins to increase abruptly and the rate of change of the pore-air pressure with the depth of wetting front at the same time is approximated by $A(\theta_c)$.

Next, let us examine the situation at the stage of $t=t_2$. According to the detailed observation under the experiment, the time t_2, that is, the time showing the point of inflection in **Fig. 5** is nearly consistent with the time when ponding begins to occur on the sand surface. So, hereafter, let us call $t=t_2$ as the ponding time and denote this ponding time as t_p. Plotting the relation between the observed depth of wetting front at the ponding time and the rainfall intensity by using a black circle, **Fig. 7** is obtained. The larger the ponding time is, the deeper the wetting
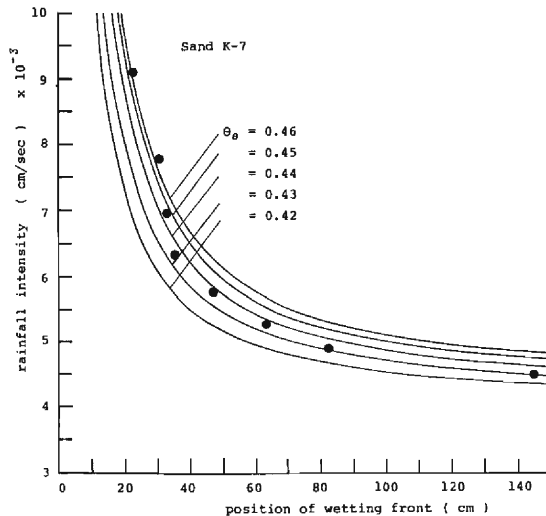

Fig. 7   Relation between the depth of wetting front and the
            rainfall intensity when ponding occurs

front advances. So, it seems from this figure that the ponding time becomes long as the rainfall intensity decreases and, especially, long enough as its intensity approaches a particular lower limiting value expected from **2.(3)**, and that this limiting value is at least less than that of the saturated hydraulic conductivity (6.5×10^{-3} cm/sec for Sand K-7). In this figure, the same relation obtained by the calculation using $\lambda = 1.5$ is also described by a groupe of curves having the various of θ_s as a parameter. Although some problems remain with the direct comparison of the observed value with the calculated one when θ_s approaches saturation as mentioned later, it seems from this figure that the observed values show similar curves to the calculated ones, and that θ_m is at least greater than θ_c (about 0.39) and near θ_{sat} (about 0.46). The result of $\theta_m > \theta_c$ gives a guarantee the result of the theoretical analysis obtained in **2.(3)**. Since the layer has practically a finite thickness, the condition when ponding occurs is to be dependent not only on the rainfall intensity but also on the thickness of layer. So, if the thickness of layer is given, the value of the critical rainfall intensity for occurring of ponding can be estimated from this figure, by using the condition that ponding occurs when the wetting front reaches the bottom.

b. moisture profile

The observed moisture profile in the case of Sand K-7 and $q = 5.29 \times 10^{-3}$ cm/sec, corresponding to **Fig. 5(a)**, is shown in **Fig. 8** by using the mass wetness, m, as a moisture content. **Fig. 9** and **Fig. 10** are the calculated moisture profile and the calculated moving velocity of particular moisture content by Eq. (51), $\partial x / \partial t$, under the same condition as **Fig. 8**, respectively. Although the moisture content near the sand surface at $t = t_p$ (about 4500 sec) cannot be estimated exactly from **Fig. 8** because of a certain degree of inaccuracy of measurement, its value becomes very large (the saturated mass wetness is 0.32–0.33). This result guarantees the result obtained from **Fig. 7** wherein θ_s at the ponding time approaches about θ_{sat}. On the other hand, when we focus the state of the moisture profile at $t = 5138$ sec in **Fig. 9**,
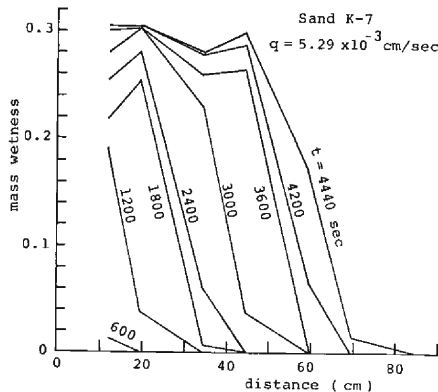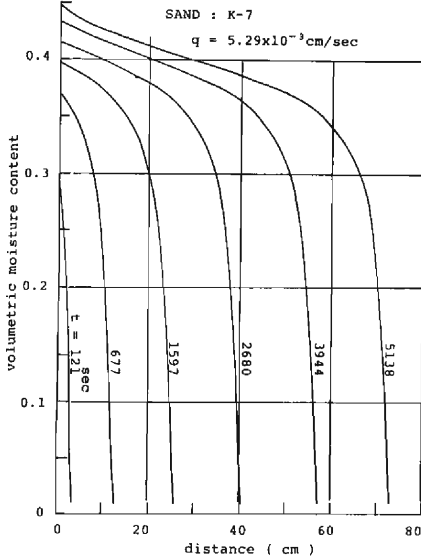

Fig. 8 Change of observed moisture profile

Fig. 9 Change of calculated moisture profile in the case of Fig. 8
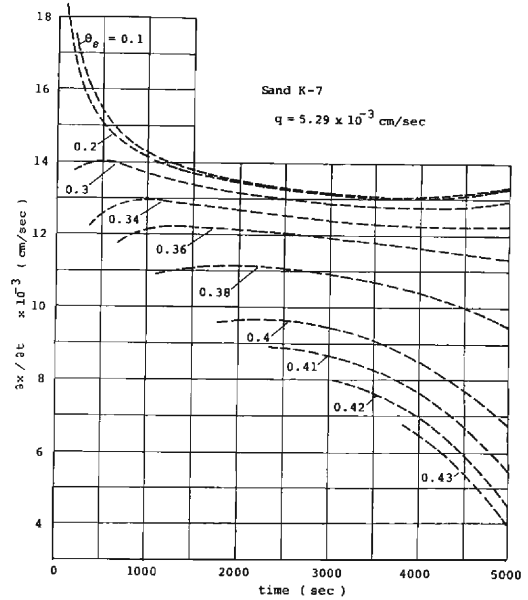
Fig. 10 Change of calculated moving velocity of particular saturation, corresponding to Fig. 9

it seems that the point of inflection appears in the part of large moisture content. And it seems from **Fig. 10** that, as time goes by, $\partial x/\partial t$ in the range of $\theta <$ about 0.36 ($\theta_c \approx 0.39$) decreases and then approaches a certain value being independent of θ, and that $\partial x/\partial t$ in the range of $\theta >$ about 0.4 decreases also and then has a very small value compared with that in the range of $\theta <$ about 0.36. This means that according to the elapsed time the transmission zone is formed and develops in the range of about $0.4 > \theta > 0.36$, and that the point of inflection appears in the moisture profile.

c. advancement of wetting front

Fig. 11(a) and **(b)** show the comparison of the observed advancement of wetting front with the calculated one by Eq. (49), where each corresponds to **Fig. 5(a)** and **(b)**, respectively. It seems from these figures that the observed values agree well with the calculated ones and the wetting front advances with a nearly constant velocity except near the beginning of an experiment. This latter point is consistent with the calculated result mentioned in **Fig. 10**.

ii) just before ponding

a. conditional equation for the quasi-saturated zone

Referring to **2.(2) (b)**, let us consider that the domain of $0 < x \leq x_1(t)$ is the quasi-saturated zone and has a particular moisture content, θ_m, and the domain of $x > x_1$ is the unsaturated zone. From this, the filter velocity of water in the quasi-saturated zone is given by
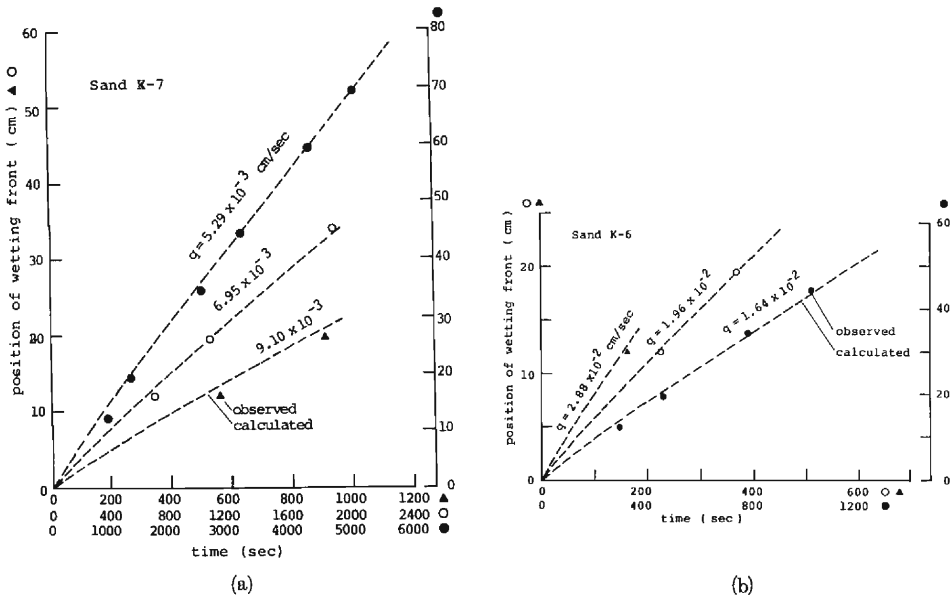
Fig. 11 Changes of the observed and calculated depths of wetting front, in the case of Fig. 5
    (a)   in the case of Sand K-7
    (b)   in the case of Sand K-6

$$\hat{v} = q \tag{58}$$

Applying Eq. (58) to the equations of movement in the quasi-saturated zone, Eq. (24) and Eq. (25), the pore-air pressure at the lower boundary of the zone and the thickness of the zone are given by

$$p_{a1} = (1 - \alpha_r) \cdot (x_1 - \psi_1 + \psi_0) \tag{59}$$

and

$$x_1 = \frac{\alpha_r \hat{K}/q}{1 - \alpha_r \hat{K}/q} \, (-\psi_1 + \psi_0) \, , \tag{60}$$

respectively, where

$$\hat{v}_a = -r(t)\hat{v} \, , \qquad (61) \qquad \alpha_r = \frac{\hat{K}_a}{\hat{K}_a + r\hat{K}} \, , \tag{62}$$

$$\psi_1 = p_{w1} - p_{a1} \, , \qquad (63) \qquad \psi_0 = p_{w0} - p_{a0} \approx p_{w0} \tag{64}$$

ψ_0 and ψ_1 are the capillary potential at $x=0$ and $x=x_1$, respectively. From Eqs. (59) and (60), the following relation is obtained.

$$\frac{p_{a1}}{x_1} = \frac{1 - \alpha_r}{\alpha_r} \cdot \frac{q}{\hat{K}} \tag{65}$$

In order to determine the profile of moisture content and pore-air pressure in

the unsaturated zone, let us approximately consider $F(\theta, t)$ defined by Eq. (29) as the F at the time when θ_s becomes θ_m, F_m. So, from Eqs. (34) and (38), the following relation is easily obtained.

$$x = x_1 - \int_\theta^{\theta_m} \frac{D(1-A)}{K(1-A)-qF_m} d\theta \tag{66}$$

$$p_a = p_{a1} + \int_\theta^{\theta_m} \frac{AD}{K} d\theta - \int_\theta^{\theta_m} \frac{AD(1-A)}{K(1-A)-qF_m} d\theta \tag{67}$$

Since F_m is a function of only θ, $(x-x_1)$ by Eq. (66) and (p_a-p_{a1}) by Eq. (67) are determined only by θ.

Therefore, the pore-air pressure at the lower boundary of a layer, p_{aL}, which can be approximated by p_a at $\theta \rightarrow 0_+$ is given by

$$p_{aL}(t) = p_{aL}(\tilde{t}) + p_{a1}(t) \tag{68}$$

where $\tilde{t}$ is the time when θ_s increases to θ_m. And by the continuity equation of water, the following relation is gotten.

$$x_1 = q \cdot (t-\tilde{t})/\theta_m \tag{69}$$

The moisture profile in $\theta < \theta_m$, of course, advances downwards unchangeably with a constant velocity, q/θ_m. Using Eqs. (68), (69) and (65), α_r defined in Eq. (62) is expressed as,

$$\frac{1}{\alpha_r} = 1 + \frac{\theta_m \hat{K}}{q^2} \cdot \frac{p_{aL}(t) - p_{aL}(\tilde{t})}{t - \tilde{t}} \tag{70}$$

and using Eqs. (59), (60) and (68), $(-\psi_1 + \psi_0)$ is expressed as

$$-\psi_1 + \psi_0 = \frac{1 - \alpha_r \hat{K}/q}{1 - \alpha_r} \{p_{aL}(t) - p_{aL}(\tilde{t})\} \tag{71}$$

b. consideration of the experimental result

Let us examine the changes of α_r and $(-\psi_1 + \psi_0)$ by using the observed pore-air pressure, p_{aL}, through Eq. (70) and Eq. (71), respectively. Since the values of $\hat{K}$ and θ_m must be determined in advance, let us define here $\hat{K}$ as the hydraulic conductivity corresponding to about 91% saturation by referring to the result of the ponded infiltration[1] and θ_m as the moisture content at $t=t_1$. So, the value of θ_m is about 0.42 for Sand K-7 from **Fig. 6**. In Sand K-6, let us consider θ_m also as 0.42.

Fig. 12(a), **(b)** and **(c)** show the changes of α_r and $(-\psi_1 + \psi_0)$ with time in the cases of Sand K-7, $q=9.10 \times 10^{-3}$ cm/sec, Sand K-7, $q=5.29 \times 10^{-3}$ cm/sec and Sand K-6, $q=1.64 \times 10^{-2}$ cm/sec, respectively, where the time axis is taken as $t-t_1$. In these figures, α_r is plotted by a black circle and $(-\psi_1 + \psi_0)$ by a white one. Especially, the values of α_r at $t=t_1$ and $t=t_2$, and the value of $(-\psi_1 + \psi_0)$ at $t=t_2$, in the
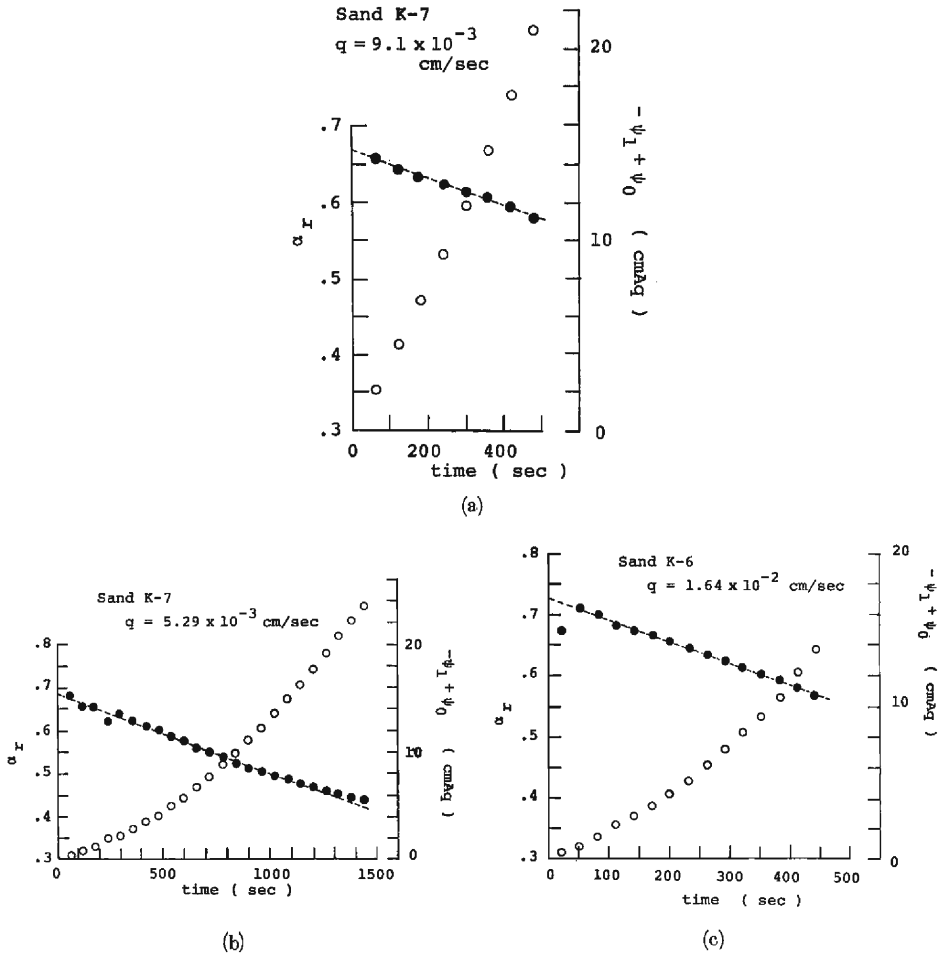
Fig. 12   Changes of α_r and $(-\psi_1+\psi_0)$
    (a)   in the case of Sand K-7 and $q=9.10\times10^{-3}$ cm/sec
    (b)   same as (a), but $q=5.29\times10^{-3}$ cm/sec
    (c)   in the case of Sand K-6 and $q=1.64\times10^{-2}$ cm/sec

case of Sand K-7, are shown in **Fig. 13**(a) and (b), respectively.   In **Fig. 13**(a), α_r are plotted by a black and a white circle at $t=t_1$ and $t=t_2$, respectively.   **Fig. 14** (a) and (b) for Sand K-6 correspond to **Fig. 13**(a) and (b), respectively.   From these figures, the following is known:

1.   Although $\alpha_r(t)$ decreases more or less linearly with time, its decrement from $t=t_1$ to $t=t_2$ is small.

2.   The values of α_r at $t=t_1$ and $t=t_2$ are about 0.7–0.6 and 0.6–0.5, respectively.

3.   The value of $(\psi_0-\psi_1)$ grows continuously.

4.   The value of $(-\psi_0+\psi_1)$ at $t=t_2$ becomes about the water entry value, ψ_e (about -20 cmAq for Sand K-7 and about -12 cmAq for Sand K-6).
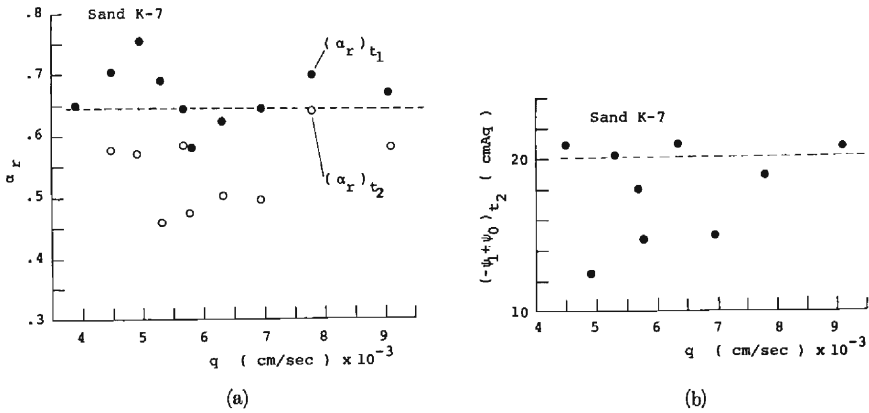
Fig. 13 (a) the values of α_r at $t=t_1$ and $t=t_2$, in the case of Sand K-7
         (b) the value of $(-\psi_1+\psi_0)$ at $t=t_2$ in the case of Sand K-7
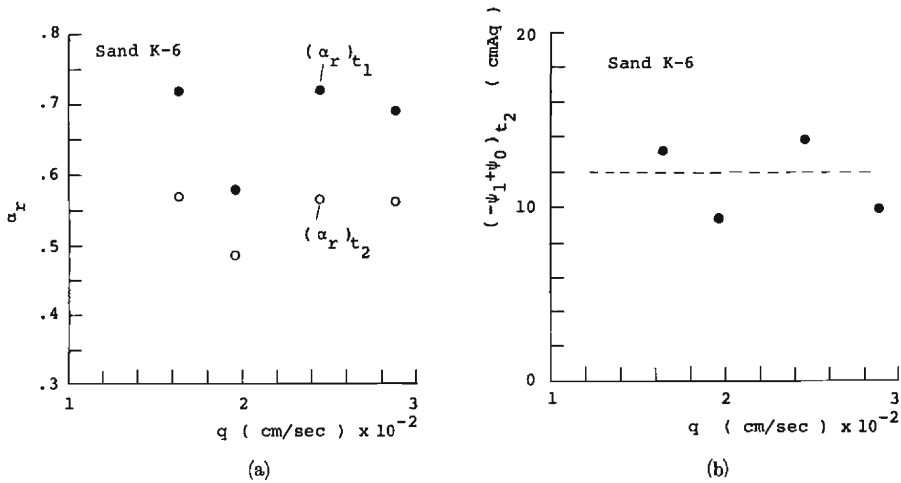

Fig. 14 (a) Same as Fig. 13 (a), but in the case of Sand K-6
         (b) Same as Fig. 13 (b), but in the case of Sand K-6

The change of α_r According to the research on ponded infiltration[1], just after the beginning of the experiment employing Sand K-7 and Sand K-6, α_r decreases abruptly from about 0.6 and then approaches a constant value, α_c(about 0.3) asymptotically.   This change of α_r is caused by the decrease of $\hat{K}_a$, that is, the increase of the resistance for the movement of pore-air through the quasi-saturated zone.

If we replace $\hat{K}$ by $K(\theta_m)$ and $\hat{K}_a$ by $K_a(\theta_m)$ in Eq. (62) at $t=t_1$ and assuming that $r=1$, we get the relation of $\alpha_r(t_1)=1-A(\theta_m)$, where $A(\theta)$ is defined in Eq. (18).   Although the value of $1-A(\theta_m)$ by using $\lambda=1.5$ in Eq. (56) for Sand K-7 is shown in **Fig. 13(a)** by a broken line, this value is not only consistent with the value of α_r at $t=t_1$ but also with that at the beginning time of the ponded infiltration mentioned above.   From these facts, we can be sure of the condition that the

quasi-saturated zone is formed after $t=t_1$. And we can state that the resistance of pore-air escape from the sand surface grows from $t=t_1$ to $t=t_2$.

The change of $(\psi_0-\psi_1)$ Since ψ_0 at the ponding time may be considered to be zero, the value of ψ_1 at that time is expected to become about the water entry value. So, we can state that, at the ponding time, the capillary potential at the lower end of the quasi-saturated zone is about the water entry value.

(c) experiment in which ponding does not occur

The change of the pore-air pressure and the depth of the wetting front in the experiment using Sand K-7 where ponding has not been observed are shown in **Fig. 15(a)** and (**b**), where each condition of the rainfall intensity is 4.21×10^{-3} and 3.29×10^{-3} cm/sec, respectively. And the calculated values according to Eq. (49) and Eq. (52) rae described also in these figures. It seems from these figures that the observed pore-air pressure changes as $d^2 p_{aL}/dt^2 > 0$ for $q=4.21 \times 10^{-3}$ cm/sec and as $dp_{aL}/dt=0$ for $q=3.29 \times 10^{-3}$ cm/sec. The observed moving velocity of wetting front in $q=3.29 \times 10^{-3}$ cm/sec seems constant. And it is concluded that all calculated values except the air pressure in $q=4.21 \times 10^{-3}$ cm/sec agree well with the observed ones.
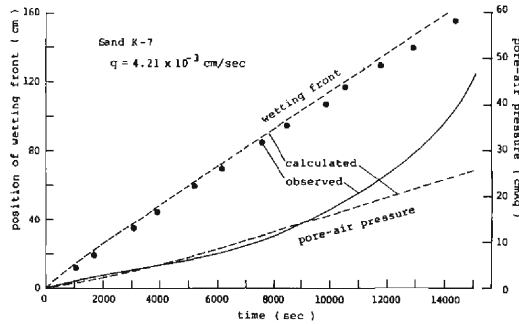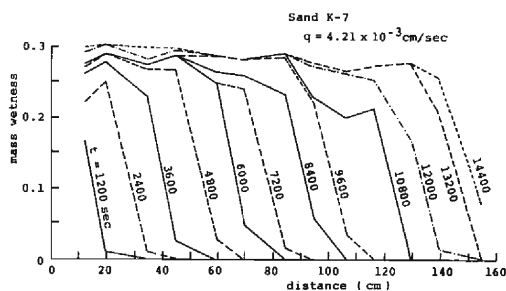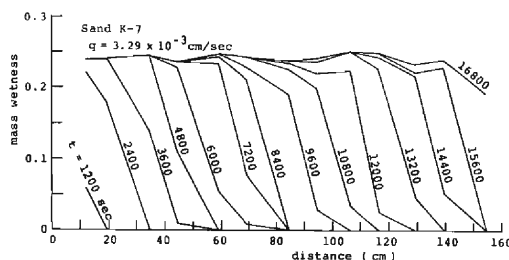

(a)
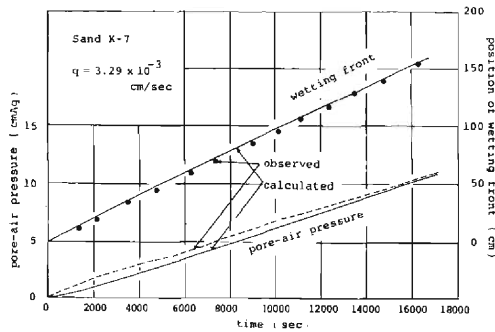
(b)

Fig. 15 Changes of the pore-air pressure and the depth
of wetting front in the case of Sand K-7
(a) $q=4.21 \times 10^{-3}$ cm/sec
(b) $q=3.29 \times 10^{-3}$ cm/sec

Fig. 16   Change of observed moisture profile
(a)   in the case of Fig. 15 (a)
(b)   in the case of Fig. 15 (b)

The observed moisture profiles are shown in **Fig. 16(a)** and **(b)**, corresponding to **Fig. 15(a)** and **(b)**, respectively. The following is observed from these figures. The moisture content near the sand surface for $q=4.21\times10^{-3}$ cm/sec increases continuously and then finally reaches a very high value. The profile exhibits the point of inflection at a relatively large moisture content and the transmission zone develops near this point with the elapsed time. On the other hand, for $q=3.29\times10^{-3}$ cm/sec, the moisture content near the sand surface reaches a nearly constant value after a relatively short elapsed time and the profile behind the wetting front exhibits $\partial\theta/\partial x=0$.

The reason why ponding does not occur is obviously based on the lack of thickness of the layer and/or the weakness of the rainfall intensity. The observed situation of the change of pore-air pressure and of the moisture profile for $q=4.21\times10^{-3}$ cm/sec are similar to those shown in article (**b**), that is, in the case where ponding is observed. The change of pore-air pressure and the advancement of the wetting front in the experiment for $q=3.29\times10^{-3}$ cm/sec are consistent with the results in Eq. (55) and Eq. (54) under the condition that $q<\{K(1-A)\}'_c$. Since the observed pore-air pressure for $q=3.95\times10^{-3}$ cm/sec is known to change as $d^2p_{aL}/dt^2>0$, we can know that the value of $\{K(1-A)\}_c$ is between 3.95×10^{-3} cm/sec and 3.29×10^{-3} cm/sec. On the other hand, estimating the value of $\{K(1-A)\}_c$ by using Eq. (56) with $\lambda=1.5$, we get about 3.9×10^{-3} cm/sec. This value satisfies the range mentioned above.

As mentioned above, the discrepancy that the calculated pore-air pressure for $q=4.21 \times 10^{-3}$ cm/sec begins to depart from the observed one with elapsed time, seems to be caused by the inaccuracy of the approximate solution mentioned in **2.(4) (c)**. For reference, the change of pore-air pressure and the advancement of the wetting front in the experiment using Sand K-6 under the condition that $q<\{K(1-A)\}'_c$ are shown in **Fig. 17**. We can also find out similar characteristic changes to **Fig. 15(b)**.
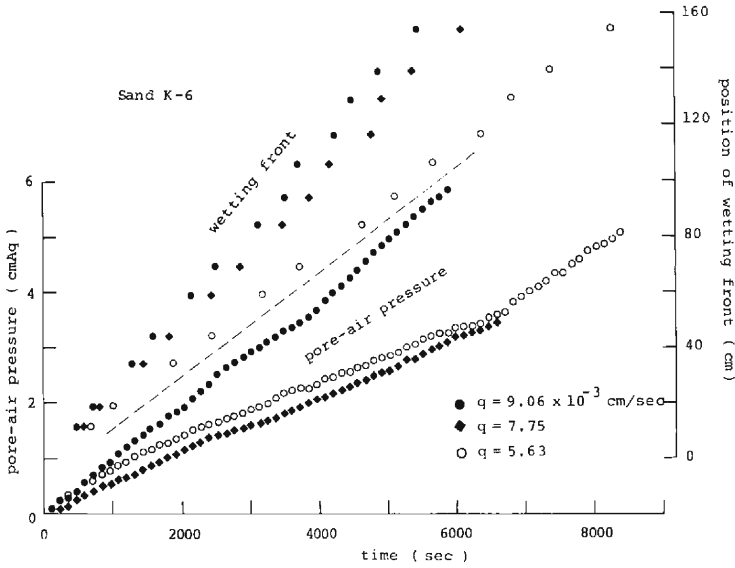
Fig. 17　Changes of the observed pore-air pressure and the depth of wetting front in the case of Sand K-6

Lastly, let us examine the permeability of pore-air in $\theta<\theta'_c$. Applying the phenomenological characteristics as shown in **Fig. 15(b)** and **Fig. 17** to Eq. (54) and Eq. (55), the permeability of pore-air at $\theta=\theta_s$ is easily given by

$$K_a(\theta) = \omega_* q \left| \frac{dp_{aL}}{dt} \right. \qquad \text{for } \theta = q/\omega_* \tag{72}$$

where θ_s is replaced by θ. The application of Eq. (72) is done as follows. In the case of Sand K-7 and $q=3.29 \times 10^{-3}$ cm/sec as shown in **Fig. 15(b)**, ω_* and dp_{aL}/dt are estimated to be 9.84×10^{-3} cm/sec and 6.17×10^{-4} cmAq/sec, respectively. Introducing these values into Eq. (72), we get $\theta=0.347$ and $K_a=5.05 \times 10^{-2}$ cm/sec. Introducing these values of θ and K_a to Eq. (56), the value of λ is 1.4. This λ-value is nearly consistent with that mentioned above.
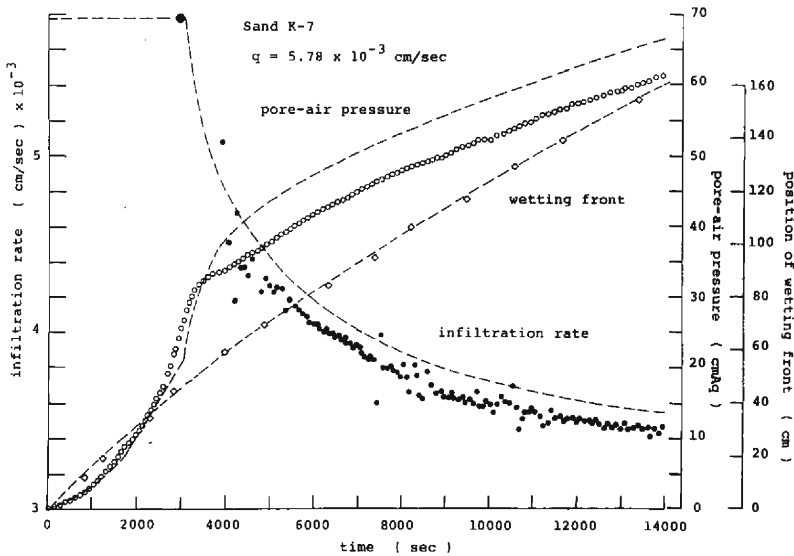
4. Infiltration after ponding

(1) Experimental result

The changes of the depth of wetting front, the pore-air pressure and the infiltration rate in the experiment using Sand K-7 are shown in **Fig. 18(a)**, **(b)** and **(c)**
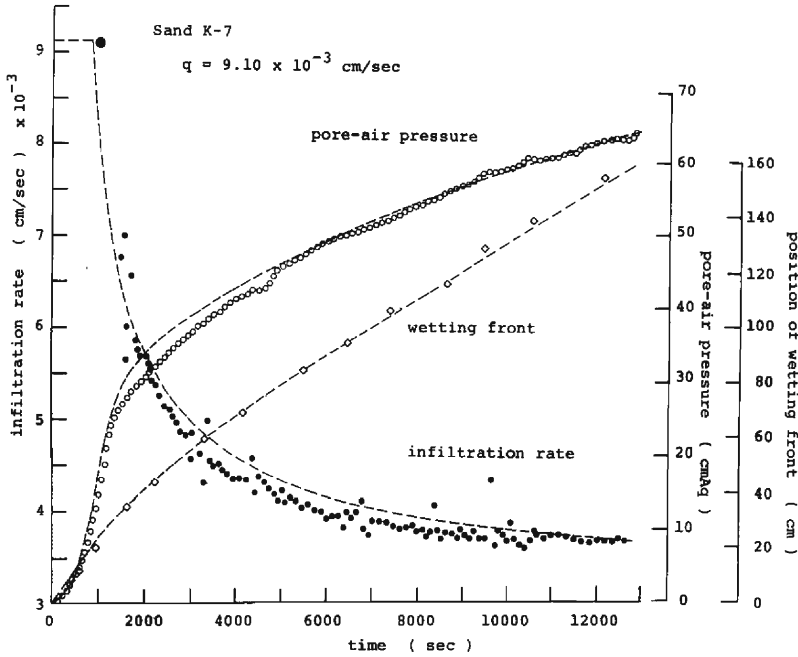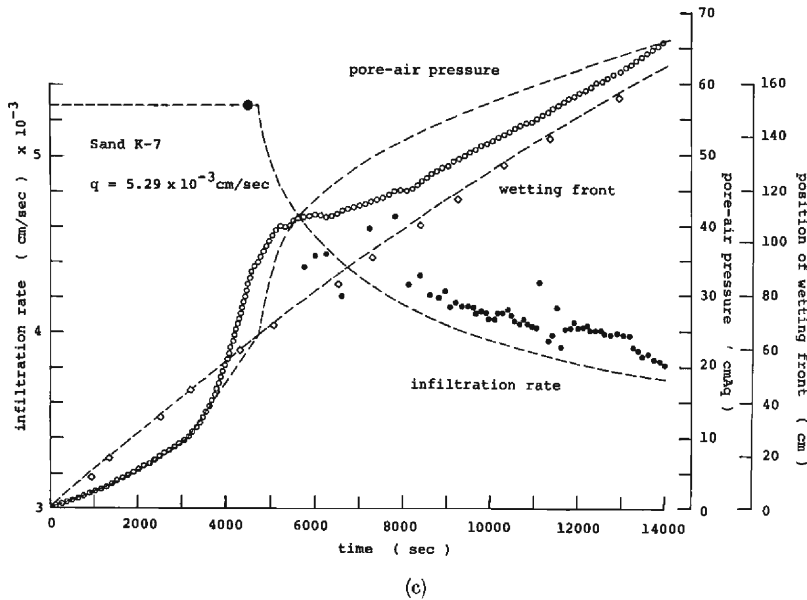

(a)

(b)

Fig. 18   Changes of the depth of wetting front, the infiltration rate and the pore-air
pressure ahead of wetting front in the case of Sand K-7
(a) $q=9.10\times10^{-3}$ cm/sec
(b) $q=5.78\times10^{-3}$ cm/sec
(c) $q=5.29\times10^{-3}$ cm/sec

by using squares, and white and black circles, respectively, where each case is under the condition of $q=9.10\times10^{-3}$, 5.78×10^{-3} and 5.29×10^{-3} cm/sec. The specially large black circle exhibits the ponding time. The meaning of the broken line described in these figure will be given later. The change of pore-air pressure described in **Fig. 18**, but during a relatively short time after ponding, is shown in **Fig. 19**. **Fig. 20** shows the observed changes of the infiltration rate and the pore-air pressure at the lower boundary of a layer in the case of the ponded infiltration[1] by using a black circle and a white one, respectively, where the layer is made of initially air-dried Sand K-7. Its thickness is 169 cm and the ponding depth is 1 cm. The ponded infiltration may be considered to correspond to the case where the rainfall intensity is sufficiently strong to the rate of infiltration capacity. The following is concluded from **Fig. 18** to **Fig. 20** and the figures of the other cases.

Infiltration rate f The infiltration rate decreases with the elapsed time as $d^2f/dt^2<0$ on the average and then approaches a particular value, f_∞, being independent of the rainfall intensity asymptotically. The value of the decreasing infiltration rate becomes smaller than 3.9×10^{-3} cm/sec mentioned in **3.**(2)(**c**), *i.e.* the value of $\{K(1-A)\}_c$ and that of the ponded infiltration shown in **Fig. 20** approaches 3.7×10^{-3} cm/sec. The changing figure, however, is similar to that of the ponded infiltration.

Pore-air pressure   The pore-air pressure increases remarkably just after the
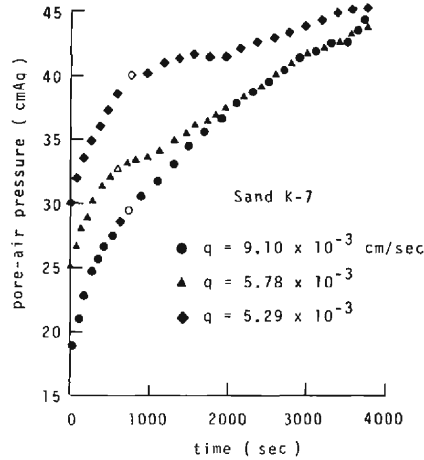
Fig. 19   Detailed figure of the pore-air pressure
shown in Fig. 18 during a relatively
short time after ponding
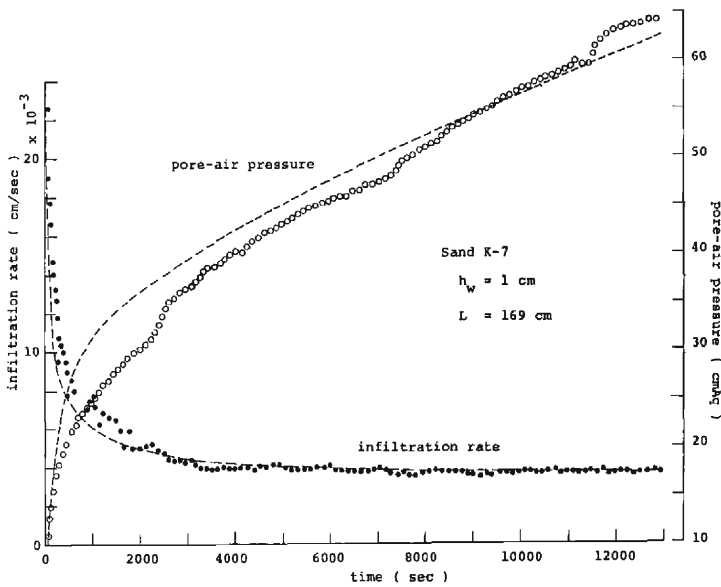
Fig. 20   Changes of the infiltration rate and the pore-air pressure at the
bottom of a layer in ponded infiltration

ponding time (roughly speaking, till the time designated by a white mark in **Fig. 19**), and then it grows moderately and finally becomes more or less linear with time. The changing figure is similar to that of the ponded infiltration.   Especially, the duration from the ponding time to the time shown by a white mark in **Fig. 19** is about constant (800 sec in Sand K-7), though its reason is not obvious.

Wetting front   The wetting front advances with decreasing moving velocity and then becomes more or less linear with time.

In the case of the ponded infiltration[1], as time goes by, the infiltration rate, the moving velocity of wetting front and the change rate of pore-air pressure ahead of the wetting front are known to be given by

$$f_\infty = \{K(1-A)\}_c ,$$ (73)

$$\omega_* = \frac{\{K(1-A)\}'_c - K_0(1-A_0)}{\theta'_c - \theta_0}$$ (74)

and

$$\dot{p}_{a\infty} = A(\theta'_c) \cdot \omega_* ,$$ (75)

respectively. In our experiment, we can replace θ_0 in Eq. (74) by zero. Therefore, in the case of Sand K-7, the values of Eq. (73), Eq. (74) and Eq. (75) are estimated on the average as 3.5×10^{-3} cm/sec, 9.5×10^{-3} cm/sec and 1.9×10^{-3} cmAq/sec[1]. For example, in the case of $q=9.10 \times 10^{-3}$ cm/sec shown in **Fig. 18(a)**, we can estimate the value of the infiltration rate, the moving velocity of wetting front and the change of pore-air pressure, after some time has proceeded, as about 3.7×10^{-3} cm/sec, about 9.7×10^{-3} cm/sec and about 2.0×10^{-3} cmAq/sec, respectively. And in the case of $q=5.78 \times 10^{-3}$ cm/sec in **Fig. 18(b)**, each value is about 3.4×10^{-3} cm/sec, about 9.0×10^{-3} cm/sec and about 2.4×10^{-3} cmAq/sec. These values seem to show that, after ponding occurs, the infiltration process and the situation of the layer become ultimately unique, regardless of the so-called initial condition at the ponding time. If the ultimate state is to be considered as strictly unique, the relations from Eq. (73) to Eq. (75) can be induced through the same theoretical analysis done by us[1] on the ponded infiltration.

(2) **Isolated pore-air**

The difference between the value of $\{K(1-A)\}_c$ expected in **3.(2)**, *i.e.* about 3.9×10^{-3} cm/sec, and that obtained in section (**1**), *i.e.* about 3.5×10^{-3} cm/sec for Sand K-7, is not much. On the other hand, the case of Sand K-6 is as follows. It was stated in **3.(2)** that the observed λ-values in Eq. (56) are scattered over a wide range, being mainly smaller than 1.9. The value of 1.9 is equal to that in the ponded infiltration[1]. If the value of $\{K(1-A)\}_c$ is estimated by using the λ-values, the value is known to be about $1.3-1.1 \times 10^{-2}$ cm/sec. Since the value of $\{K(1-A)\}_c$ estimated in the ponded infiltration is about 1.1×10^{-2} cm/sec, the difference of both values of $\{K(1-A)\}_c$ is also not much. However, this inconsistency brings to us the interesting problem from the phenomenological point of view. Let us examine why this inconsistency appears.

Since $\{K(1-A)\}_c$ is dependent on the hydraulic conductivity and the permeability of pore-air, the inconsistency is obviously caused by the change of these factors. The change of the permeability of pore-air may be based on the change of the existing situation of the air in the layer. That is, in detail, it is caused by changing the

free pore-air, which has existed dominantly in the layer up till ponding occurs, into the so-called isolated pore-air, to some extent, because, after the ponding time, the pore-air becomes easily confined by the penetrating water compared with before that time. On the other hand, the change of hydraulic conductivity may be considered to be caused by the change of the passing route of a penetrating water[12] and by the development of the dead-water zone, corresponding to the occurrence of the isolated pore-air. Although it is not easy to take simultaneously into consideration the effect of the change of two factors on $\{K(1-A)\}_c$, let us consider, as a first approximation, that only the occurrence of the isolated pore-air has any responsibility for this inconsistency of the values of $\{K(1-A)\}_c$.

It is known in section (**1**), that, as time goes by, the infiltration process becomes a kind of the stationary state, and, furthermore, that in the ponded infiltration the moisture profile behind the moving wetting front, being in the range of $\theta < \theta'_c$, becomes nearly unchangeable[1]. Referring to these evidences, let us consider, at first, such a situation wherein the movement of the penetrating water and the state of the formed isolated pore-air are stationary in a domain of a layer having the larger scale compared with Darcy's scale. Denoting the volumetric isolated pore-air content as θ'_a, the relation between θ and θ'_a can be assumed as follows.

$$\theta'_a = \kappa_\infty \cdot \theta \tag{76}$$

where κ_∞ is a numerical constant value. This relation corresponds to the assumption, that, when the complicated network of pores in a sand layer is considered to be composed of many pore-channels with the same magnitude in diameter as that of pores, the probability compelling the free pore-air in each channel to become isolated is constant for each channel.

Denoting the volumetric free pore-air content as θ^e_a, θ^e_a is given by

$$\theta^e_a = \theta_{sat} - \theta - \theta'_a \tag{77}$$

Since the permeability of free pore-air in the stationary state, $K_{a\infty}$, may be considered to be the function of θ^e_a, the following equation is obtained by using Eq. (76) and Eq. (77) and by referring to Eq. (56).

$$K_{a\infty} = K(\theta_{sat}) \frac{\mu_w}{\mu_a} \cdot \Phi \left(1 - \delta_\infty \frac{\theta}{\theta_{sat}} \right) \tag{78}$$

where $$\delta_\infty = 1 + \kappa_\infty \tag{79}$$

and $1 \geq \Phi \geq 0$. When the Φ can be expressed by the power function of $(1 - \delta_\infty \theta / \theta_{sat})$ under consideration of Eq. (56), Eq. (78) is rewritten by

$$K_{a\infty} = K(\theta_{sat}) \frac{\mu_w}{\mu_a} \left(1 - \delta_\infty \frac{\theta}{\theta_{sat}} \right)^{\lambda_*} \tag{80}$$

where λ_* is a positive numerical constant. Especially, in the case of $\delta_\infty = 1$, i.e., $\kappa_\infty = 0$, Eq. (80) is equal to Eq. (56).

In our previous paper[1] with respect to the ponded infiltration, the effect of the isolated air on the flow resistance of pore-air is represented by putting, for example, $\delta(\tau) = 1$ and $\lambda_* = 1.8$ for Sand K-7 in Eq. (111) to be mentioned later. Since, in the case of infiltration of a rainfall, $\delta(\tau)$ must be considered to change with time, it is impossible to describe that effect by using $\delta(\tau) = 1$ and $\lambda_* = 1.8$ for Sand K-7. Therefore, in this paper, $\delta(\tau)$ changing with time and $\lambda_* = 1.5$ for Sand K-7 being equal to that in the infiltration without ponding are available for analysis.

Let us examine the relation between $\{K(1-A)\}_c$ or θ_c and δ_∞ by using Eq. (80) as the function of K_d and by taking λ_* as a parameter. The example of the case of Sand K-7 is shown in **Fig. 21**. It is known from this figure that $[\partial\{K(1-A)\}_c/\partial\delta_\infty]_{\lambda_*} < 0$ and $[\partial\theta_c/\partial\delta_\infty]_{\lambda_*} < 0$. Paying attention to the curve showing the relation between $\{K(1-A)\}_c$ and δ_∞ for $\lambda_* = 1.5$, the value of $\{K(1-A)\}_c$ at $\delta_\infty = 1$ is estimated to be about 3.9×10^{-3} cm/sec as mentioned in **3.(2) (c)**. And the value of δ_∞ for $\{K(1-A)\}_c = 3.5 \times 10^{-3}$ cm/sec corresponding to the final infiltration rate is also estimated to be about 1.06. Although this value is a little smaller than that usually known[11], the estimated value can be considered reasonable. It can be understood, therefore, that the discrepancy of the value of $\{K(1-A)\}_c$ is mainly based on the effect of the increase of the isolated pore-air in the layer.
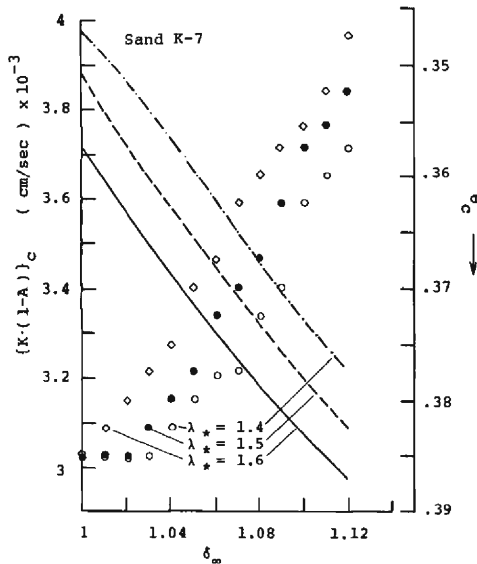

Fig. 21 Relation between $\{K(1-A)\}_c$ or θ_c and δ_∞ for the various values of parameter λ_*

(3) Modification of fundamental equations for the unsaturated zone

(a) fundamental equation

Let us consider how the fundamental equation for the unsaturated zone shown in **2.(2)** is modified by taking into account the problem of isolated pore-air.

i)   continuity equation

The continuity equation for water, Eq. (11), is obviously held unchanged.

The continuity euqation for pore-air given by Eq. (12) is rewritten as

$$\frac{\partial \rho_a^e \theta_a^e}{\partial t} + \frac{\partial \rho_a' \theta_a'}{\partial t} + \frac{\partial \rho_a^e v_a}{\partial x} = 0 \tag{81}$$

where ρ_a^e and ρ_a' are the density of free air and isolated air, respectively.

Especially, in the case where the effect of the dead water becomes a serious problem, considering θ in Eq. (11) as the moisture content including the dead-water, Eq. (11) is also obvious.

ii)   equation of motion

The equations of motion for water and free pore-air are also given by the generalized Darcy's law and are rewritten as

$$v = -D(\theta)\frac{\partial \theta}{\partial x} + K(\theta) \cdot \left(1 - \frac{\partial p_a^e}{\partial x}\right) \tag{82}$$

and

$$v_a = -K_a(\theta_a^e) \cdot \left(\frac{\partial p_a^e}{\partial x} - \frac{\rho_a^e}{\rho_w}\right), \tag{83}$$

respectively, where

$$D(\theta) = K(\theta) \cdot \frac{d(p_w - p_a^e)}{d\theta} \tag{84}$$

and p_a^e is the increment of free pore-air pressure over the atmospheric pressure.

Furthermore, in the case where the effect of dead-water becomes a serious problem, considering the θ in Eq. (82) and Eq. (84) as the moisture content excluding the dead-water, Eq. (82) and Eq. (84) are held unchanged[13].

iii)   state equation of air

The state equation of air given by Eq. (13) is rewritten for the free pore-air and the isolated pore-air by

$$\rho_a^e = C \cdot (P_{a0} + p_a^e) = C \cdot P_a^e \tag{85}$$

and

$$\rho_a' = C \cdot (P_{a0} + p_a') = C \cdot P_a', \tag{86}$$

respectively, where p_a' is the increment of the isolated air pressure over the atmospheric pressure, P_{a0}, on the average.

(b)   approximation of the fundamental equation

From the fundamental equation obtained in article (a), using the boundary conditions at $x=L$, Eq. (3) and Eq. (4), $\partial p_a^e/\partial x$ corresponding to Eq. (14) is given by

$$\frac{\partial p_a^e}{\partial x} = -\frac{A^e D}{K}\frac{\partial \theta}{\partial x} + A^e\left(1 - \frac{\rho_a^e}{\rho_w}\right) - A^e \varepsilon^e + \frac{\rho_a^e}{\rho_w} - A^e \varepsilon' \tag{87}$$

where

$$\varepsilon^e = \int_x^L (\theta_{sat} - \theta) \frac{\partial P_a^e}{\partial t} dx / K \bar{P}_a^e , \tag{88}$$

$$\varepsilon' = \int_x^L \frac{\partial}{\partial t} \{(P_a^e - P_a')\theta_a'\} dx / K \bar{P}_a^e , \tag{89}$$

$$\bar{P}_a^e(t) = P_a^e(x, t) - \Delta p_a^e(x, t) , \tag{90}$$

$$\bar{P}_a^e \gg |\Delta p_a^e| \tag{91}$$

and

$$A^e = \frac{K(\theta)}{K(\theta) + K_a(\theta_a^e)} . \tag{92}$$

Let us make an approximation for the second and the fourth terms in the right side of Eq. (87) by A^e and 0, respectively, by the same reason mentioned earlier in **2.(2)**. And, referring to the result of the ponded infiltration[1], the third term, $A^e \varepsilon^e$, may be approximated as zero, excluding the stage just after ponding. Since, furthermore, the contribution of the fifth term on $\partial p_a^e / \partial x$ may be not considered so much, Eq. (11) and Eq. (87) become approximately as follows, respectively.

$$\frac{\partial \theta}{\partial t} = \frac{\partial}{\partial \lambda} \left\{ D(1 - A^e) \frac{\partial \theta}{\partial x} - K(1 - A^e) \right\} \tag{93}$$

$$\frac{\partial p_a^e}{\partial x} = -\frac{A^e D}{K} \frac{\partial \theta}{\partial x} + A^e \tag{94}$$

After all, the effect of isolated pore-air on the fundamental equation for the unsaturated zone is expressed as the modification of A defined in Eq. (18) by A^e in Eq. (92). We call Eq. (93) and Eq. (94) newly as the modified approximate fundamental equation for the unsaturated zone.

Especially, the filter velocity in this case is expressed by

$$v = -D(1 - A^e) \frac{\partial \theta}{\partial x} + K(1 - A^e) \tag{95}$$

As time goes by, $K(\theta_a^e)$ or $A(\theta_a^e)$ becomes the function of θ only. Thus, the fact that the final infiltration rate is equal to $\{K(1 - A^e)\}_c$ can be easily obtained by the same method as that used for the ponded infiltration[1].

(4) Solution of the modified fundamental equation

(a) solution for the unsaturated zone with parameters defined at its upper end

According to Eq. (26) and by using Eq. (95) and Eq. (5), the function F in this case is expressed by

$$F = \frac{-D(1 - A^e) \left/ \frac{\partial x}{\partial \theta} \right. + K(1 - A^e) - K_0(1 - A_0)}{f - K_0(1 - A_0)} \tag{96}$$

where the initial moisture content, θ_0, is to be about zero in this case and so A_0^e is replaced by A_0.

Following the analysis[1] on the ponded infiltration after a long elapsed time, the F at such a stage is given by

$$F = \frac{\theta - \theta_0}{\theta_c' - \theta_0} \frac{\{K(1-A^e)\}_c' - K_0(1-A_0)}{\{K(1-A^e)\}_c - K_0(1-A_0)} \quad \text{for} \quad \theta < \theta_c' \tag{97}_1$$

$$F = \frac{K(1-A^e) - K_0(1-A_0)}{\{K(1-A^e)\}_c - K_0(1-A_0)} \quad \text{for} \quad \theta_c' < \theta < \theta_c \tag{97}_2$$

$$F = 1 \quad \text{for} \quad \theta > \theta_c \tag{97}_3$$

Since θ_c is nearly equal to θ_c' as known from **Fig. 1** because of $\theta_0 \approx 0$, for the convenience of analysis, let us approximate Eq. (97) as follows.

$$F = \frac{\theta}{\theta_c} \quad \text{for} \quad \theta < \theta_c$$
$$F = 1 \quad \text{for} \quad \theta > \theta_c \tag{98}$$

According to the approximation mentioned in **3.(2) (b)**, F is given at the ponding time, t_p, by

$$F = \frac{\theta}{\theta_m} \tag{99}$$

Since the F at $\theta = \theta_c$, i.e., F_c, must be equal to θ_c/θ_m at $f = q$ from Eq. (99) and 1 at $f = f_\infty$ from Eq. (98), let us consider, as a first approximation, the relation between F_c and $f(t)$ as follows.

$$F_c = \frac{\theta_c}{\theta_m} + \left(1 - \frac{\theta_c}{\theta_m}\right) \frac{q-f}{q-f_\infty} \tag{100}$$

As shown in **Fig. 22** where the dotted and the broken lines mean the F at $t = t_p$ and $t \to$ infinity, respectivley, let us assume that the function $F(\theta, t)$ is given by the two straight lines through F_c. That is,
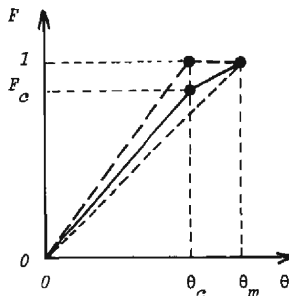

Fig. 22 Figure of function F

$$F = \frac{\theta}{\theta_c} F_c \qquad \text{for} \quad \theta < \theta_c$$

$$F = \frac{\theta - \theta_c}{\theta_m - \theta_c} + F_c \frac{\theta_m - \theta}{\theta_m - \theta_c} \quad \text{for} \quad \theta > \theta_c \tag{101}$$

Especially, θ_c described in **Fig. 22** decreases with time and approaches a particular value asymptotically.

Using Eq. (100) and Eq. (101), the solution of approximate fundamental equation for the unsaturated zone is easily obtained as follows.

Introducing Eq. (101) into Eq. (96), the moisture profile is given by

$$x = x_1 - \int_\theta^{\theta_m} \frac{D(1 - A^e)}{K(1 - A^e) - fF} d\theta \tag{102}$$

where $x_1(t)$ is the depth of the lower boundary of quasi-saturated zone, and θ_m is θ at $x = x_1$, being considered to be constant.

Using Eq. (102) to Eq. (94), the profile of free pore-air pressure is given by

$$p_a^e = p_a^e(\theta_m, t) + \int_\theta^{\theta_m} \frac{A^e D}{K} d\theta - \int_\theta^{\theta_m} \frac{A^e K(1 - A^e)}{K(1 - A^e) - fF} d\theta \tag{103}$$

Since Eq. (102) and Eq. (103) must satisfy the continuity equation of water, the following conditional equation is obtained.

$$q t_p + \int_{t_p}^t f dt = \theta_m x_1 - \int_0^{\theta_m} \frac{\theta D(1 - A^e)}{K(1 - A^e) - fF} d\theta \tag{104}$$

Eq. (104) is the equation which determines the change of infiltration rate.

(b) solution for the quasi-saturated zone with parameters defined at its lower end

From the fundamental equation for the quasi-saturated zone, Eq. (24) and Eq. (25), the filter velocity of water and the pore-air pressure at the lower end of this zone can be given by[1]

$$\hat{v} = \alpha_r \hat{K} \left(1 + \frac{\beta_r / \alpha_r}{x_1} \right) \tag{105}$$

and

$$p_{a1} = (1 - \alpha_r) \cdot (x_1 + \beta_r / \alpha_r) + p_{w0}, \tag{106}$$

respectively, where

$$\beta_r = \alpha_r(-\psi_1 + p_{w0} - p_{a0}) \approx -\alpha_r \psi_1, \tag{107}$$

and α_r and ψ_1 are defined in Eq. (62) and Eq. (63), respectively.

(5) Comparison between the observed result and the calculated one

(a) determination of the unknown parameter

i) α_r and β_r

The value of α_r at ponding time is about 0.55 for Sand K-7 and Sand K-6 as mentioned in **3.(2)**. And the change of the values of α_r for ponded infiltration was also stated in **3.(2)**. α_r may be approximated by α_r at $r=1$, $\alpha(t)$, except just after ponding time[1]. So, if we do not pay attention to the stage just after ponding, the change of $\alpha(t)$ can be given approximately by

$$\alpha(t) = \alpha_c + (\alpha_0 - \alpha_c)e^{-b(t-t_p)} \tag{108}$$

where α_0 is α at ponding time, and b a positive numerical constant defined as follows. The stage where the pore-air pressure ahead of the wetting front is increasing abruptly just after ponding, as mentioned in section **(1)**, may be considered to correspond to that for the quasi-saturated zone being formed but not developing enough[1]. So, for the purpose of calculation later, let us conveniently determine the value of b as the half-life of $\alpha(t)$ which is equal to the one-fourth of the duration of that stage mentioned in section **(1)** (about 800 sec in the case of Sand K-7).

On the other hand, $\beta_r(t)$ is as follows. Referring to the result of the ponded infiltration that $\beta_r(t)$ is held nearly constant, it is expressed by[1]

$$\beta_c = -\alpha_c\psi_e/(1-\alpha_c) \tag{109}$$

So, β_r can be expressed approximately as follows.

$$\beta_r = \beta_c \tag{110}$$

ii) θ_m and $\hat{K}$

According to **3.(2)**, the value of θ_m is given by that of θ_s at $t=t_2$. The value of $\hat{K}$ is given by $K(\theta)$ at 91% saturation.

iii) $K_a(\theta_a^e)$

After ponding occurs, the rate of the volume occupied by the isolated pore-air in the layer is expected to grow and ultimately becomes stationary as mentioned in section **(2)**. For the stage before ponding occurs, we gave the permeability of pore-air by Eq. (80) replacing δ_∞ by 1. At the stage when time has proceeded enough after ponding occurs, we used Eq. (80) in section **(2)**. Now, it becomes a problem how the function of K_a changes between $t=t_p$ and $t \to \infty$. Considering both boundary conditions, let us assume $K_a(\theta, t)$ to be as follows.

$$K_a(\theta, \tau) = K(\theta_{sat})\frac{\mu_w}{\mu_a}\left\{1 - \delta(\tau)\frac{\theta}{\theta_{sat}}\right\}^{\lambda_*} \tag{111}$$

where

$$\delta(\tau) = \delta_\infty + (\delta_0 - \delta_\infty)e^{-a\tau}, \tag{112}$$

$\tau = t - t_p$, and λ_* is equal to λ_* in Eq. (80) and also λ in Eq. (56). δ_0 is δ at $t=t_p$,

i.e., 1, and a is a positive numerical constant. Eq. (111) under the condition of Eq. (112) is considered to have the following phase. The value of K_a for the particular θ, $K_a(\tau; \theta)$, decreases with time and this means that, as time goes by, the isolated pore-air is easily formed. Considering the approach to Eq. (80) based on Eq. (76) and Eq. (77), we get the relation $\theta_a' = \{\delta(\tau) - \delta_0\}\theta$ being similar to Eq. (76), where $\{\delta(\tau) - \delta_0\}$ corresponds to κ_∞ in Eq. (76), then grows and ultimately becomes κ_∞.

The values of δ_∞ and a in Eq. (112) are as follows. The value of δ_∞ is determined by using the conditional equation, Eq. (73). On the other hand, the value of a cannot be estimated *a priori* but this can be determined by a trial and error method as the calculated pore-air pressure ahead of the wetting front shows a good agreement with the observed one.

iv) p_{w0}

According to the result of the ponded infiltration[1], the water pressure at the upper boundary of a layer, p_{w0}, is approximated by the ponding depth to a high degree of accuracy.

(b) examples of calculation

By calculation, the infiltration rate, $f(t)$, can be determined from Eq. (104) and Eq. (105). The moisture profile can be determined from Eq. (102) and Eq. (105) by using the obtained $f(t)$. Finding out p_{w0} in Eq. (106), the profile of free pore-air pressure can be determined from Eq. (103) and Eq. (106) by using the obtained $f(t)$ and $x_1(t)$.

The calculated values of the infiltration rate, the depth of wetting front having $\theta = 0.2$ and the free pore-air pressure ahead of the wetting front in Sand K-7 are shown in **Fig. 18(a)**, **(b)** and **(c)** by the broken line, where, as the maximum ponding depth in the experiment is only about 0.5 cm as mentioned in **3.(1)**, p_{w0} in the calculation is set at zero approximately. In these calculations, we get $\delta_\infty = 1.06$–1.08 and $a = (\ln 0.5)/3600\ \text{sec}^{-1}$, corresponding to that the half-life of δ in Eq. (112) is about 1 hr. Especially, although the calculated value before ponding is described in these figure, these are as follows. The calculated value till θ_s reaches θ_m, that is, $t < t_1$, follows the solution in the second approximation mentioned in **2.(4)**. On the other hand, for $t_1 < t < t_p$: x_1 at $t = t_p$ is determined from Eq. (105). And t_p and p_{a1} at $t = t_p$ are determined from Eq. (69) and Eq. (106) by using the known $x_1(t_p)$, respectively. So, referring the result obtained in **3.(2)**, the calculated value is given by connecting these at $t = t_1$ and $t = t_p$ with a straight line.

It is known from these figures that the calculated values agree well with the observed ones. This means that the physical-mathematical model after ponding is satisfactory to express the infiltration process. And it is concluded that, even when the rainfall intensity changes after the ponding time, the model is applicable unchanged under the condition that the ponding depth exists only on the sand surface. However, the pore-air pressure must be changed linearly according to the change of the ponding depth.

5. Equation of the infiltration capacity

In this chapter, let us consider the simplified equation to determine the change of infiltration rate, that is, the so-called law of infiltration for engineering use, though it loses a small degree of accuracy.

(1) Conditions for the law of infiltration

In order to derive a simplified law of infiltration, the following conditions are assumed by referring to the results obtained above.

i)   field and rainfall

1.   Eq. (1) to Eq. (6) are satisfied, but after ponding, the change of rainfall intensity causes no trouble as long as a pond exists on the ground surface.   Therefore, even the occurrence of a lateral flow is of no relevance.

2.   The hydraulic conductivity and the permeability of pore-air are unchanged with time and space.   So, we do not directly consider the occurrence of isolated pore-air and dead-water.

3.   The zone having $\theta = \theta_0$ always exists ahead of the downward advancing wetting front.

ii)   before ponding

1.   The function F defined in Eq. (29), F_{be}, obeys either of the following: in the case of $\theta_s \leq \theta_c^*$

$$F_{be} = \frac{\theta - \theta_0}{\theta_s - \theta_0} \tag{113}_1$$

in the case of $\theta_s > \theta_c^*$

$$F_{be} = \frac{\theta - \theta_0}{\theta_c^* - \theta_0} \quad \text{for} \quad \theta_0 < \theta \leq \theta_c^*$$
$$= 1 \quad \text{for} \quad \theta > \theta_c^* \tag{113}_2$$

where θ_c^* is θ satisfying the condition of

$$\frac{\theta - \theta_0}{\theta_c' - \theta_0} = \frac{\{K(1-A)\}_c - K_0(1-A_0)}{\{K(1-A)\}_c' - K_0(1-A_0)} \tag{114}$$

and $\theta_c' < \theta_c^* < \theta_c$.   The F_{be}, only in $\theta_m > \theta_s > \theta_c^*$, is inconsistent with the F in Eq. (48). So, the application of Eq. (113) is expected to make θ_s grow faster in comparison with that of Eq. (48).

2.   After θ_s reaches θ_m, the moisture profile advances downwards unchanged. So, its moving velocity is equal to $\{q - K_0(1-A_0)\}/(\theta_m - \theta_0)$.

iii)   after ponding

1.   The function F defined in Eq. (96), F_{af}, obeys

$$F_{af} = \frac{\theta - \theta_0}{\theta_c^* - \theta_0} \quad \text{for} \quad \theta_0 < \theta < \theta_c^*$$
$$= 1 \quad \text{for} \quad \theta > \theta_c^* \tag{115}$$

Eq. (115) corresponds to the approximated relation of Eq. (97) and is consistent with Eq. (113)$_2$.

2. α_r defined in Eq. (62) and β_r defined in Eq. (107) are held constant, and each is equal to α_c and β_c defined in Eq. (109), respectively.

(2) Derivation of the equation

From using the continuity equation for water, Eq. (113) and Eq. (29), the time when θ_s increases to θ_m, t_1, is given by

$$t_1 = -\frac{\displaystyle\int_{\theta_0}^{\theta_m} d\theta \int_{\theta}^{\theta_m} \frac{D(1-A)}{K(1-A)-K_0(1-A_0)-F_{be}\{q-K_0(1-A_0)\}} d\theta}{q-K_0(1-A_0)} \tag{116}$$

The ponding time, t_p, is given from Eq. (105) and the conditions 2. in ii) and iii) by

$$t_p = t_1 + (\theta_m - \theta_0)\frac{\beta_c \hat{K}}{q-\alpha_c \hat{K}} \Big/ \{q-K_0(1-A_0)\} \tag{117}$$

Using Eq. (116) and Eq. (117), the relation between f and t can be obtained as follows. Arranging Eq. (96) with respect to $\partial x/\partial \theta$ and integrating it with respect to θ yields

$$x = x_1 - \int_{\theta}^{\theta_m} \frac{D(1-A)}{K(1-A)-K_0(1-A_0)-F_{af}\{f-K_0(1-A_0)\}} d\theta \tag{118}$$

where x_1 is given by the function of f from Eq. (105). The integration of $\partial x/\partial t$ obtained from Eq. (118) with respect to θ in the range between θ_{0+} and θ_m is equal to $\{f-K_0(1-A_0)\}$ due to the continuity equation for water. So, after integrating this conditional equation with respect to t, the law of infiltration is given as follows.

$$t = t_p + G_{qs} + G_{us} \tag{119}$$

where

$$G_{qs} = \frac{(\theta_m-\theta_0)\beta_c \hat{K}}{K_0(1-A_0)-\alpha_c \hat{K}}\left[\frac{1}{f-\alpha_c \hat{K}} + \frac{1}{K_0(1-A_0)-\alpha_c \hat{K}}\ln\left|\frac{f-K_0(1-A_0)}{f-\alpha_c \hat{K}}\right|\right]_f^q$$
$$\text{for}\quad K_0(1-A_0) \neq \alpha_c \hat{K} \tag{120}$$

$$= -\left[\frac{(\theta_m-\theta_0)\beta_c \hat{K}}{4(f-\alpha_c \hat{K})^4}\right]_f^q \qquad \text{for}\quad K_0(1-A_0) = \alpha_c \hat{K}$$

$$G_{us} = \int_{\theta_0}^{\theta_m} d\theta \int_{\theta}^{\theta_m} \frac{D(1-A)F_{af}}{K(1-A)-K_0(1-A_0)}\cdot\left[\frac{1}{K(1-A)-K_0(1-A_0)(1-F_{af})-fF_{af}}\right.$$
$$\left. + \frac{1}{K(1-A)-K_0(1-A_0)}\ln\left|\frac{f-K_0(1-A_0)}{K(1-A)-K_0(1-A_0)(1-F_{af})-fF_{af}}\right|\right]_f^q d\theta$$

$$\tag{121}$$

$[\cdots]_f^q$ in Eq. (120) and Eq. (121) means $[\cdots]_{f=q} - [\cdots]_{f=f}$.

As known from Eq. (119), the change of infiltration rate is expressed implicitly. However, from Eq. (119), we can easily estimate the elapsed time for an arbitrary infiltration rate under the condition that $q > f > \{K(1-A)\}_c$.
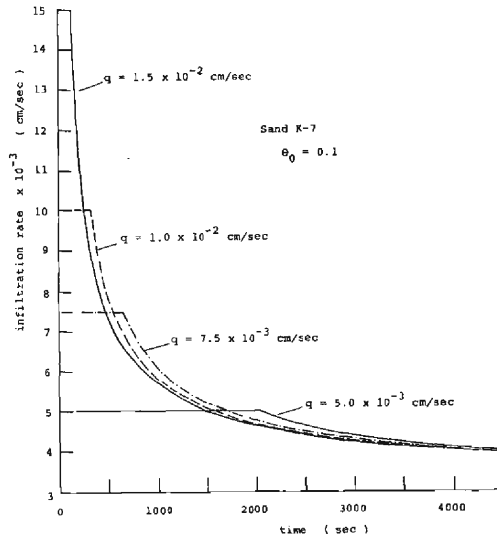
(a)
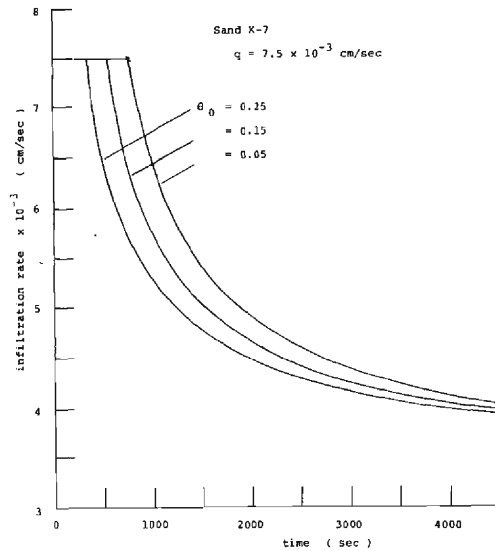
(b)

Fig. 23   Change of calculated infiltration rate
(a)   in the case that q is variable but θ_0 is constant
(b)   in the case that θ_0 is variable but q is constant

(3) Examples of calculation

The effects of the rainfall intensity, q, and the initial moisture content, θ_0, on the change of infiltration rate are shown in **Fig. 23(a)** and **(b)**, respectively, where these calculations are done for Sand K-7 in the range of $\alpha_c \hat{K} > K_0(1-A_0)$, and the former case is in case of $\theta_0 = 0.1$ and the latter case is in case of $q = 7.5 \times 10^{-3}$ cm/sec. The final or ultimate infiltration rate is taken to coincide with the results of experiment as $f_\infty = \{K(1-A)\}_c = 3.5 \times 10^{-3}$ cm/sec. It seems from these figures that, as time goes by, the infiltration rates after ponding eventually change along a particular curve being independent of the values of rainfall intensity and the initial moisture content, and that the smaller the initial moisture content is, the longer the ponding time becomes.

Up till now, several simple formulae with respect to the law of infiltration have been proposed. Among them, there are the equation based on the Green & Ampt model[14] or the delta function model presented by Philip (1957)[15], the same type of equation as this but having the new physical interpretation to the included parameters by Morel-Seytoux and Khanji (1974)[16], the equation by Philip (1975)[15], and the Horton's type of equation given a physical background by Ishihara and Ishihara (1962)[17]. However, the effect of the movement of pore-air on penetrating water is ignored in these, except for the equation by Morel-Seytoux *et al.*, where
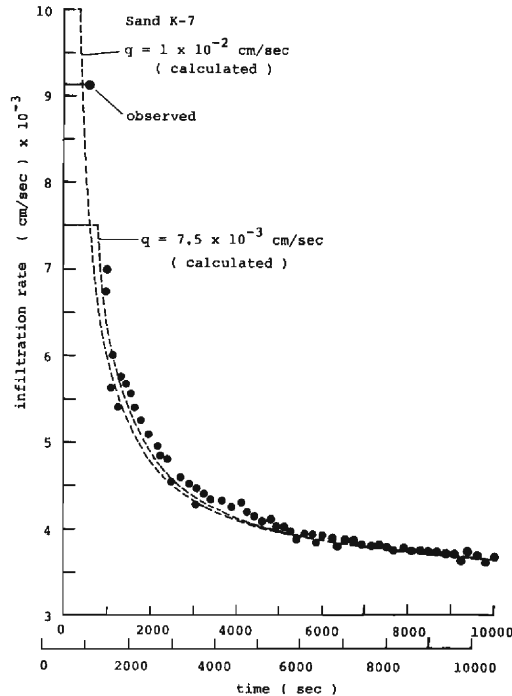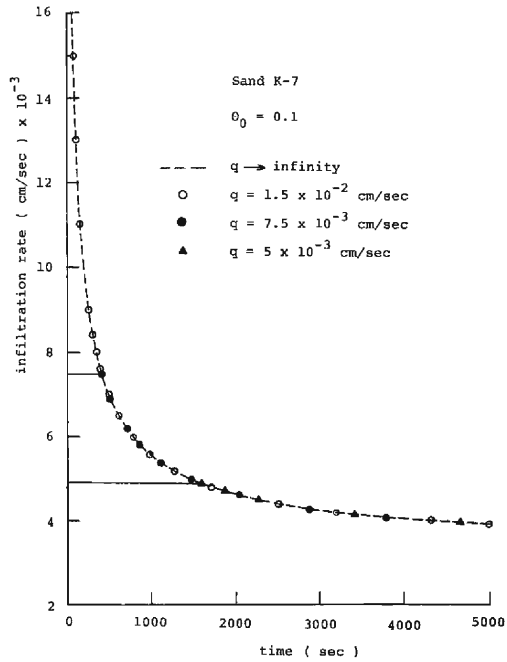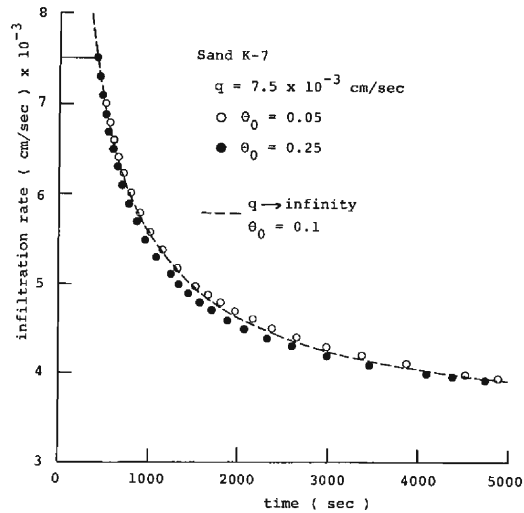

Fig. 24   Comparison of the calculated infiltration rate
with the observed one

(a)

(b)

Fig. 25   Curves of the calculated infiltration rate after
          shifting the time
          (a)   same as Fig. 23 (a)
          (b)   same as Fig. 23 (b)

the condition is that the pore-air ahead of a wetting front is at atmospheric pressure.

The most interesting point on the law of infiltration for an engineering hydrologist is how the infiltration rate decreases with time and how much the final infiltration rate, f_∞, is.

According to the above discussion, the final infiltration rate, f_∞, under the condition that pore-air is possible to escape throughout a ground surface is given by $\{K(1-A)\}_c$ which is estimated as about half of the hydraulic conductivity in saturation $K(\theta_{sat})$. On the other hand, it is seen, in **Fig. 23(a)** and **(b)**, that all the curves show a very similar phase. Then, after shifting the time axis, the comparison of results calculated by Eq. (119) with that obtained by experiment on $q=9.10\times 10^{-3}$ cm/sec is shown in **Fig. 24**, where the lower time axis is for the experiment and a large black circle corresponds to the experimental ponding time. Agreement between them is very good. Furthermore, making similar time shifts, **Fig. 23(a)** and **(b)** become **Fig. 25(a)** and **(b)**, respectively. Although a slight deviation can be observed in **Fig. 25(b)**, all the curves overlap each other very well. For engineering purpose, applying a simple equation to these overlapped curves under the consideration that the final infiltration rate f_∞ becomes $\{K(1-A)\}_c$, the following formula is obtained.

$$\begin{aligned} f &= c(t+t_0)^{-n} \quad &\text{for} \quad t \leq t_c \\ &= f_\infty \quad &\text{for} \quad t > t_c \end{aligned} \tag{122}$$

where t is the elapsed time after ponding under the condition that q_p is the rainfall intensity at the beginning of ponding, n a positive numerical constant determined by the kind of sand, c a numerical constant determined also by the kind of sand, $t_0=(q_p/c)^{-1/n}$ and $t_c=(f_\infty/c)^{-1/n}-t_0$. The standard figure of the change of infiltration rate being similar to the equation of Kostiakov (1932)[18] is shown for Sand K-7 in **Fig. 26** by two straight lines, where a black circle is the calculated value of Eq. (119).
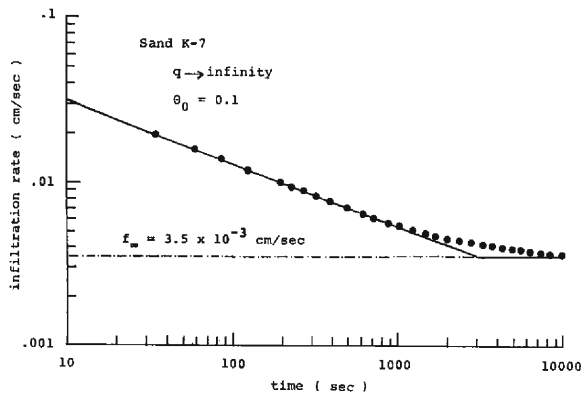

Fig. 26 Standard figure of the change of infiltration rate with time

6. Conclusion

The infiltration process of a rainfall with constant intensity into a homogeneous layer initially having a uniform moisture profile was explored theoretically and experimentally.

The results obtained are summarized as follows:

1) When the rainfall intensity, q, is greater than the maximum value, $\{K(1-A)\}_c$, of $K(1-A)$, there is the possibility for the occurrence of ponding on the surface of a layer.

Before ponding:

2) In the case of $q < \{K(1-A)\}_c$, the moisture content, θ_s, at the surface of a layer grows and then approaches the lesser moisture content, $\tilde{\theta}$, satisfying the condition of $q = K(1-A)$.

Especially, in $q < \{K(1-A)\}'_c$, as time proceeds, the wetting front eventually advances downwards with an unchangeable profile and a constant moving velocity, $\omega_* = \{q - K_0(1-A_0)\}/(\tilde{\theta} - \theta_0)$, where θ_0 is the initial moisture content. The pore-air pressure ahead of the wetting front increases linearly with time after a relatively short elapsed time.

3) In the case of $q > \{K(1-A)\}_c$, θ_s grows and then reaches about 90% saturation, θ_m, at a certain time. During this process, the pore-air pressure ahead of the wetting front changes as its second differentiation with respect to time is positive, and changes remarkably, especially after θ_s becomes θ_m.

4) After θ_s has become θ_m, a quasi-saturated zone is formed downwards from the upper boundary of a layer. At that stage, α_r defined by $\hat{K}_a/(\hat{K}_a + r\hat{K})$ decreases almost linearly with time from 0.7–0.6 to 0.6–0.5 for both Sand K-7 and Sand K-6. Although the decrement is small, this decrease is cuased by the increase of resistance against the movement of pore-air throughout that zone. The difference in capillary potential at each boundary of quasi-saturated zone, $(\psi_0 - \psi_1)$, grows and becomes about the minus sign of the water entry value at the ponding time. That is, at that time, the capillary potential at the lower boundary of quasi-saturated zone, ψ_1, becomes nearly the water entry value.

After ponding:

5) As time goes by, isolated air is formed in the layer and finally becomes stationary. At the stationary stage, the volumetric free pore-air content, θ_a^s, is given by $\theta_{sat} - \delta_\infty \theta$, where θ is the volumetric moisture content and $\delta_\infty = 1.06$–1.08 for Sand K-7.

6) Regardless of the condition in the layer at ponding time, after some time, the phase of infiltration becomes nearly uniquely determined, this condition being same as that in ponded infiltration.

7) The law of infiltration after ponding is proposed by Eq. (119) and, for engineering use, by Eq. (122).

Acknowledgements

References

1) Ishihara, Y. and E. Shimojima: A role of pore air in infiltration process, Bull. Disast. Prev. Res. Inst., Kyoto Univ., Vol. 33, Part 4, 1983, pp. 163–222.

2) Ishihara, Y., F. Takagi and Y. Baba: Experimental study on the vertical infiltration of rainwater, Disast. Prev. Res. Inst., Kyoto Univ., Annuals, No. 9, 1966, pp. 551- 563 (in Japanese).

3) McWhorter, D.B.: Infiltration affected by flow of air, Hydrology Papers, Colorado State Univ., 1971.

4) Corey, A.T.: Mechanics of heterogeneous fluids in porous media, Water Resources Publications, 1977, pp. 202–210.

5) Phuc, L.V. and H.J. Morel-Seytoux: Effect of soil air movement and compressibility on the infiltration rates, Soil Sci. Amer. Proc., Vol. 36, 1972, pp. 237–241.

6) Sonu, J. and H.J. Morel-Seytoux: Water and air movement in a bounded deep homogeneous soil, J. Hydrology, Vol. 29, 1976, pp. 23–42.

7) *e.g.* Mein, R.G. and C.L. Larson: Modeling infiltration during a steady rain, Water Resources Res., Vol. 9, 1973, pp. 384–394.

8) Philip, J.R.: On solving unsaturated flow equations: 1, The flux-concentration relation, Soil Sci., Vol. 116, 1973, pp. 328–335.

9) Philip, J.R. and J.H. Knight: On solving the unsaturated flow equations: 3, New quasi-analytical technique, Soil Sci., Vol. 117, 1974, pp. 1–13.

10) Parlange, J.Y.: The theory of water movement in soil: 8, One-dimensional infiltration with constant flux at the surface, Soil Sci., Vol. 114, 1972, pp. 1–4.

11) *e.g.* Scheidegger, A.E.: The physics of flow through porous media, Univ. of Toronto Press, 3rd ed., p. 255.

12) Wilson, L.G. and J.N. Luthin: Effect of air flow ahead of the wetting front on infiltration, Soil Sci., Vol. 96, 1963, pp. 136–143.

13) Philip, J.R.: The theory of absorption in aggregated media, Aust. J. Soil Res., Vol. 6, 1968, pp. 1–30.

14) *e.g.* Childs, E.C.: An introduction to the physical basis of soil water phenomena, A Wiley-Interscience Publication, 1969, pp. 275–277.

15) Philip, J.R.: The theory of infiltration:4. Sorptivity and algebraic infiltration equations, Soil Sci., Vol. 84, 1957, pp. 257–264.

16) Morel-Seytoux, H.J. and J. Khanji: Derivation of an equation of infiltration, Water Resources Res., Vol. 10, 1974, pp. 795–800.

17) Ishihara, T. and Y. Ishihara: Recent development of runoff analysis —Mainly in the Yura river—, Annuals, Disast. Prev. Res. Inst., Kyoto Univ., Vol. 5–B, 1962, pp. 33–58 (in Japanese).

18) *e.g.* same as 14), but pp. 278–279.

Appendix

The moisture profile in the zone of $\theta_{s\infty} > \theta > \theta_*$ under the condition of $q > \{K(1-A)\}_c$

Let us consider the figure of moisture profile in $\theta_{s\infty} > \theta > \theta_*$ under the assumption of no ponding.

The moisture profile in $\theta_{s\infty} > \theta > \theta_{s\infty} - \Delta$, where Δ is a certain small positive value: If the moisture profile fixed in space is assumed to exist in $\theta_{s\infty} > \theta > \theta_n (\geq \theta_*)$, F defined in Eq. (29) is equal to one in the zone due to the continuity equation of water, Eq. (23), and v given by Eq. (21) is equal to $\{K(1-A)\}_{n+}$ at $\theta = \theta_{n+}$, where the suffix n means the value at $\theta = \theta_n$, because $1/(\partial x/\partial \theta)$ becomes zero at $\theta = \theta_{n+}$. However, since v_{n+} is less than q, because of $q > \{K(1-A)\}_c$, the continuity of water is not maintained. Therefore, the moisture profile in $\theta_s > \theta > \theta_{s\infty} - \Delta$ is known to be prolonged in space. In such a zone, the relation of Eq. (45) is, of course, satisfied.

The moisture profile in $\theta_* < \theta < \theta_* + \Delta$: The existence of fixed moisture profile is shown to be impossible by applying to Eq. (21) the conditions that v in this zone is equal to $\{K(1-A)\}_*$ and $\partial\theta/\partial x$ is negative. So, the moisture profile in this zone is known to be also prolonged. Now, Since $\partial x/\partial t$ at $\theta = \theta_{*+}$ and $\theta = \theta_{*-}$ must be physically consistent each other, it is known from Eq. (40), Eq. (45) and the definition of θ_c' such a condition that θ_* is consistent with θ_c'.

The moisture profile in the intermediate moisture content between $\theta_{s\infty}$ and θ_*: Since the moisture profiles are prolonged, at least, in $\theta_{s\infty} > \theta > \theta_{s\infty} - \Delta$ and $\theta_* < \theta < \theta_* + \Delta$, the profile in the zone of intermediate moisture content between $\theta_{s\infty}$ and θ_* is known to move. So, let us assume the existence of a zone shown by the advancing front with an unchangable moisture profile and a constant velocity like the wetting front in this domain. In such a case, the always prolonging moisture profiles are connected to the advancing front at its both ends. Denoting the moisture contents at these ends as $\theta_n^{(1)}$ and $\theta_n^{(2)} (> \theta_n^{(1)})$, the velocity of front is given from our previous paper[*] by $[\{K(1-A)\}_n^{(2)} - \{K(1-A)\}_n^{(1)}]/(\theta_n^{(2)} - \theta_n^{(1)})$, being similar to that of wetting front shown in Eq. (40), where the suffixes $_n^{(1)}$ and $_n^{(2)}$ mean the values at $\theta = \theta_n^{(1)}$ and $\theta = \theta_n^{(2)}$, respectively. Although this velocity must be physically consistent with $\partial x/\partial t$ given by Eq. (45) at $\theta = \theta_{n+}^{(2)}$, it is known that the consistency is impossible by the definition of $\theta_c' (= \theta_*)$ and the shape of function $K(1-A)$. As a result, the moisture profile in the intermediate zone between $\theta_{s\infty}$ and θ_* is also prolonged.

After all, it is concluded that the moisture profile in $\theta_{s\infty} > \theta > \theta_*$ is prolonged.

[*] Ishihara, Y. and E. Shimojima: A role of pore air in infiltration process, Bull. Disast. Prev. Res. Inst., Kyoto Univ., Vol. 33, part 4, 1983, pp. 163–222.